University of Calgary

PRISM Repository **https://prism.ucalgary.ca**

The Vault Open Theses and Dissertations

2022-12-06

Body Composition Features in Colorectal Cancer: Clinical Outcomes and Biological Factors

Armstrong, Victoria Suzanne

Armstrong, V. S. (2022). Body composition features in colorectal cancer: clinical outcomes and biological factors (Master's thesis, University of Calgary, Calgary, Canada). Retrieved from https://prism.ucalgary.ca. http://hdl.handle.net/1880/115581

Downloaded from PRISM Repository, University of Calgary

UNIVERSITY OF CALGARY

Body Composition Features in Colorectal Cancer: Clinical Outcomes and Biological Factors

by

Victoria Suzanne Armstrong

A THESIS

SUBMITTED TO THE FACULTY OF GRADUATE STUDIES

IN PARTIAL FULFILMENT OF THE REQUIREMENTS FOR THE

DEGREE OF MASTER OF SCIENCE

GRADUATE PROGRAM IN MEDICAL SCIENCE

CALGARY, ALBERTA

DECEMBER, 2022

© Victoria Suzanne Armstrong 2022

Abstract

Background: Cancer is a global health burden and a leading cause of death worldwide. One obstacle to improving patient outcomes is the development of cancer cachexia, which is formally described as the loss of muscle tissue (with or without adipose tissue atrophy). The classical presentation of cachexia is low muscle mass (sarcopenia) which can be assessed by computed tomography (CT) image assessment techniques, but this may not embody all important body composition phenotypes. I hypothesize that cancer can induce multiple clinically significant body composition (BC) features beyond sarcopenia, such as myosteatosis and high subcutaneous fat density (dense sub-q).

Methods: In a cohort of patients with stage I – IV colorectal cancer (CRC) (N = 319), BC features were measured using Slice-O-Matic CT image analysis techniques. The influence of BC phenotypes and other clinical parameters on overall survival (OS) outcomes was assessed using univariate Kaplan-Meier and multivariate Cox regression analyses. Findings were then validated on an external dataset of 960 patients with CRC. To explore the physiological basis of these BC features, I performed targeted serum proteomics using Luminex assays and untargeted shotgun tumor proteomics using liquid chromatography-mass spectrometry.

Results: Overall, the three BC features (sarcopenia, myosteatosis and dense sub-q) appeared independent of one another in 60% of cases. Myosteatosis and dense sub-q were independent predictors of worse OS outcomes ($P < 0.001$, $P = 0.050$). Sarcopenia was influential on reducing OS when phenotypic overlap was removed ($P = 0.002$). Several perturbed protein correlates were found in relation to each BC phenotype, specifically with respect to inflammation and metabolic

processes. For example, myosteatosis was independently associated with increased leptin, resistin and adipsin ($P < 0.01$ for all).

Conclusion: Overall, this work demonstrates that colorectal cancer can lead to the development of several BC phenotypes beyond just muscle wasting. Distinct patterns of serum protein abundance suggested that each of the BC features represented biologically distinct manifestations.

Acknowledgements

I would like to thank several people for their contributions to my research and for their continued support over these past few years. First and foremost, I would like to thank my supervisor, Dr. Oliver Bathe, for his continued guidance, encouragement and expertise throughout the course of my research. Thank you to my committee members, Dr. Anthony MacLean and Dr. Paul Beck, for their insights and guidance over the last few years. Thank you to our collaborators from the Dufour Lab, specifically to Dr. Antoine Dufour, Luiz Gustavo Almeida and Daniel Young for providing me with their support and expertise. And finally thank you to my lab members for your continued support and collaboration, specifically Cynthia Stretch, Jennifer Koziak, Jannat Pervin, Jodi Rattner, Elleine Allapitan, Nico Boelter, Liam Fitzgerald, Robab Hassanvand Jamadi and Pedram Torabian.

Table of Contents

List of Figures

List of Tables

Chapter 1: Introduction

1.1 Cancer Burden

In 2020, cancer continued to represent a global health burden and a leading cause of worldwide morbidity and mortality (1). Specifically, there were over 19.3 million new cases diagnosed and 10 million cancer-associated deaths in 2020 alone, making this disease a major public health challenge and threat to increasing life expectancy (1). It has been projected that by 2040 there will be a 47% increase in the incidence of cancer cases, which is linked closely to continued population growth and aging (1).

Particularly troublesome cancer types are colorectal cancers (CRCs). GLOBOCAN 2020 reported that CRCs had the third overall highest incidence and were the second leading cause of cancer mortality, worldwide (1). Dichotomized by sex in 2020, CRC was the second most common cancer type in females (behind breast) and third most common in cancer type in males, behind prostate and lung (1).

1.1.1 Risk Factors

There are several modifiable and non-modifiable risk factors that increase the likelihood of developing CRC. One non-modifiable risk factor includes a positive family history for CRC. Positive familial history of CRC, which is linked to approximately 10 – 20% of all CRC cases, varies widely between families and relies on factors such as the number of the family members with disease and the severity of disease cases (2). Family history of CRC is different, however, from another non-modifiable risk factor for CRC development which is the presence of hereditary CRC syndromes. Hereditary CRCs are inherited syndromes that increase the risk of CRC development

(3). Such conditions are rare and responsible for between 5 – 7% of all CRC cases and can be largely categorized into non-polyposis (limited or no polyps, such as Lynch Syndrome) or polyposis syndromes (lots of polyps, such as Familial Adenomatous Polyposis) (3, 4). Other non-modifiable factors such as older age (especially over the age of 50) and the presence of inflammatory bowel diseases (i.e. ulcerative colitis and Crohn's disease) also increase the risk of CRC development (1).

Modifiable risk factors are largely responsible for the development of sporadic (no genetic predisposition) CRCs, which comprise ~ 70% of cases diagnosed (5). Risk factors that increase the likelihood of sporadic CRC development include: a sedentary lifestyle, heighted consumption of red and processed meats, excess body weight, alcohol consumption and cigarette smoking (1). Both modifiable and non-modifiable risk factors increase the likelihood of CRC development. The quintessential route to CRC development involves polyps transitioning from benign to malignant.

1.1.2 CRC Pathogenesis

Polyps are localized growths of abnormal cells that, with time, can accumulate genetic mutations that drive them towards malignancy. Progression of precancerous polyps to cancer is a relatively slow process that can take years to occur, which highlights the importance for screening (6). The transition from benign growths to cancerous ones is related to augmented genomic instability, which is a staple of all cancer development. In CRC, there are generally three pathogenic pathways that lead to the development of two types of polyps: adenomas and sessile serrated polyps (SSPs) (7). Adenomatous polyps are precursors for ~ 60 – 70% of new CRC cases, and SSPs are linked to 25 – 30% of new cases (6).

Adenomas are associated with a large degree of chromosomal instability, which is a genetic imbalance wherein there are significant gains or losses of large sections of chromosomes (5). These rearrangements often lead to the activation of oncogenes *KRAS* and *BRAF*, or the inactivation of tumor suppressing genes like *APC* and *TP53* and loss of chromosome 18 heterozygosity (8). Loss of heterozygosity (LOH) refers to the loss of two alleles of a gene. These changes often lead to loss-of-function of tumor suppressing genes, such as *DCC*, *SMAD2* and *SMAD4* (8). The culmination of these specific changes are key features of the adenoma-carcinoma sequence.

SSPs typically develop through *BRAF* (sometimes KRAS) gene mutations which causes uncontrolled cellular growth and loss of apoptosis (6). *BRAF* mutations are also associated with another condition in CRC development known as CpG island methylator phenotype (CIMP). CIMP leads to the hypermethylation of gene promotors, which can silence tumor suppressor genes and can also impact other genes that regulate growth promotion (6, 9).

The third mechanism that is frequently observed in CRC development is microsatellite instability (MSI), typically culminating in CRC derived from SSPs (6). MSI is caused by defective DNA mismatch repair wherein there is uneven replication of microsatellites, which are short stretches of repetitive, noncoding DNA sequences (10). Uneven replication with no repair mechanisms available heighten the likelihood that genetic mutations may occur. MSI is also a feature of hereditary, non-polyposis conditions such as Lynch Syndrome (7).

As described above, CRCs exemplify a large degree of heterogeneity in terms of etiology and pathogenesis. The molecular phenotypes of CRC have been widely categorized into tumor

markers, which are related MSI or DNA mismatch repair, CIMP and somatic mutations in BRAF/KRAS (11). The heterogeneity of these phenotypes have important implications for CRC prognosis and clinical management (11).

1.1.3 Treatment Regimens for CRC

Despite advances in treatment options for CRC, no universal treatment exists that is appropriate for every case of CRC. Surgical resection with curative intent remains the primary goal in all CRC cases (7). Surgical resection can be supplemented with chemotherapy and radiation depending on disease stage and anatomical factors. For instance, early stage disease usually allows for favorable conditions for tumor resection without any neoadjuvant (before surgery) treatments, such as chemotherapy or radiation (7). However, complete resection of the tumor is not always a viable option, especially in late-stage disease. In some advanced stage situations, neoadjuvant chemotherapy (or chemoradiation) can be given to a shrink tumor(s) that are not initially appropriate for resection, to make surgical resection a viable option (12). Often in advanced stage IV, where surgical resection is not an option, palliative chemotherapy is offered (13, 14).

The chemotherapeutic agents that are utilized in CRC include cytotoxic and cytostatic drugs (15). There are several class of targeted therapy, including angiogenesis inhibitors (e.g., bevacizumab) and epidermal growth factor (EGF) inhibitors (e.g., cetuximab). Angiogenesis inhibitors block new blood vessel formation through the inhibition of vascular endothelial growth factor (VEGF) (16).

Cytotoxic drugs include a wide range of drugs, such as fluorouracil/leucovorin, capecitabine, irinotecan and oxaliplatin (15). The mechanisms of action of each drug range from inhibition of cellular division via DNA fragmentation to activation of programmed cell death (15). Often chemotherapy treatment plans combine different combinations of these drugs, such as FOLFIRI (irinotecan, leucovorin and fluorouracil) or FOLFOX (oxaliplatin, fluorouracil and leucovorin) (15).

While chemotherapeutic treatments are effective therapeutic options that are frequently utilized for CRC cancer, radiation is only used for rectal cancers, due to the complicated pelvic anatomy (7). For instance, radiation can be used as a neoadjuvant treatment with the goal of shrinking the size of the tumor before resection (17). Additionally, radiation can used both during surgery (intraoperative radiation therapy) or postoperatively to help kill any remaining cancer cells and reduce the likelihood of recurrence (17).

Although a wide variety of treatment options are available to patients with CRC, not all treatments are effective in every patient. There are numerous chemoresistance mechanisms (18). Ultimately, with numerous lines of chemotherapy, cumulative toxicities take hold and patients decline. Moreover, some chemotherapies can lead to cachexia, which has been consistently shown to increase the risk of toxicity of treatment in cancer settings (19).

1.1.4 Cancer Therapy Contributes to Cancer Cachexia

Cancer cachexia, by international consensus, is defined as skeletal muscle loss with or without the loss of adipose tissue (20). Drivers of this condition include inflammation and perturbed energy balance. There is also increasing evidence that some forms of chemotherapy

can contribute to the development and progression of cachexia (19). Cachexia, in turn, can enhance intolerance to treatment and reduce treatment effectiveness.

The main etiologies behind chemotherapy-induced cachexia are still under investigation, and there may be several pathogenic mechanisms. 5-fluorouracil has been shown to promote a negative nitrogen balance in tumor-bearing rats (21). Barreto et al. (2016) demonstrated that combination therapy FOLFIRI promotes wasting through activation of p38 mitogen-activated protein kinases and ERK1/2 pathways (independent of the ubiquitin proteasome system) (22). Most recently, Pin et al. (2019) revealed via comprehensive metabolic profiling of a murine Colon26 adenocarcinoma mouse model that cancer-induced and FOLFIRI chemotherapy-induced cachexia had substantially different metabolic derangements and inflammatory processes (19).

1.2 Cancer Cachexia

Cancer cachexia is a complex disorder which manifests in a variety of cancer types, and consistently reduces survival outcomes compared to cancer patients who do not exhibit cachectic wasting (23). The degree of muscle/adipose tissue wasting does not depend on the size of the tumor, which adds another dimension of complexity (24). It is thought that severe metabolic demands by the tumor, in addition to a systemic inflammatory response, are drivers. Other factors such as reduced food intake, enhanced catabolism and elevated resting energy expenditure also make this disorder distinct from starvation (19).

Models of cancer cachexia demonstrate that this disorder involves several organs such as the pancreas, liver, heart, skeletal muscle and adipose tissue (23). Each organ is influenced by the development of cachexia, which further adds to the difficulty in developing appropriate

therapeutic responses. Ultimately, building blocks such as amino acids and free fatty acids are released (from skeletal muscle and adipose tissue, respectively) and mobilized into the circulation which may represent fuels for the metabolic demands of the tumor (23). The liver is also involved in providing additional fuel sources, largely through the conversion of lactate into glucose, which is shunted back to the tumor for energy utilization (23). Such processes create a negative energy balance driven by these tumor-related metabolic demands, in addition to the onset of cancer-related anorexia symptoms (20). Often this wasting is 1) both difficult to halt once started and 2) cannot be fully reversed by supplementary nutritional support (20).

1.3 Assessing Cachexia and Body Composition Phenotypes

The techniques for detecting the presence of cachexia have been previously discussed in detail (20). There are three specific methods of assessing cancer cachexia, which are either by a weight loss of > 5% over 6 months, a BMI < 20, or through a low appendicular skeletal muscle index (SMI), known as sarcopenia in conjunction with weight loss > 2% (20). The latter method's assessment of sarcopenia is made possible through the use of techniques such as computed tomography (CT) imaging. Throughout the course of treatment for cancer, CT imaging is conducted as it plays an important role in tumor staging and treatment planning (25). As such, analytic tools that allow for the extraction body composition information from CT images (such as skeletal muscle/adipose tissue surface area and radiodensity) have been developed.

1.4 Body Composition Assessment Techniques

The measurement of body composition phenotypes in patients with cancer is critical in cachexia research (26). Despite the continued advocacy for routine assessment of muscle mass

and strength in cachexia research, a lack of consensus regarding body composition measurement methodology still exists. The most commonly utilized method is CT (and sometimes MRI) cross-sectional assessment, which are valuable because they allow for an accurate segmentation of fat and fat-free mass (27). Other measures of body composition assessment, such as duel-energy x-ray absorptiometry (DXA), anthropometric measurements and bioelectrical impedance have also been used, but to a lesser extent (20).

Whole body CT images are constructed using helical CT scanners that combine and stacked X-ray images (at different planes) into series of two dimensional (2D) images (27). The 2D transaxial images, typically at the level of the third lumbar vertebra, are used for evaluating the muscle and fat characteristics of patients with cancer in a cross-sectional manner. In this technique, the axial images are submitted to software such as Slice-O-Matic for body composition analysis which quantifies both muscle and adipose tissue surface area. Additionally, due to the inherent characteristics of CT images, muscle and adipose tissue radiodensity can also be assessed through the Hounsfield Unit (HU) scaling system, which makes CT images advantageous over MRI images which lack the radiodensity component (27). The HU system can detect the radiodensity of the pixels within the CT images (28). For instance, intramuscular lipid content can be measured through pixel density, as lower density pixels in the muscle region correspond to higher lipid content (as lipids are less dense than muscle) (28). In a similar manner, density of adipose tissue can also be conducted. As a benefit, these measures can be completed at no additional cost if CT images from a patient's course of treatment are utilized. Contrast media used during image capture, as well as slice thickness, are both factors to consider in BC assessment as they can influence pixel densities (29).

CT image assessment has made the evaluation of body composition in cancer more attainable in research settings. Arguably the most commonly assessed phenotype detectable by CT image analysis is sarcopenia, which is well described in the literature. This well-documented BC phenotype is the "classical" definition of cancer cachexia and is influential in reducing overall and disease-free survival in cancer (30). Cancer-associated sarcopenia has also been shown to increase the likelihood of treatment toxicity in patients with cancer and increases frailty (31). However, as result of utilizing CT measurement techniques, several other body composition (BC) "phenotypes" have been documented that go beyond low appendicular skeletal muscle index (sarcopenia).

Another BC phenotype has more recently come to light. , Myosteatosis (lipid accumulation in skeletal muscle tissue) appears on CT as low radiodensity muscle. This phenotype has been described as biologically distinct from sarcopenia and is influential on survival outcomes of patients with cancer (32). Myosteatosis, along with a very recently described phenotype known as highly dense adipose tissue, are both prevalent in cancer populations and therefore require further examination (33, 34). The discovery of additional, influential body composition features may suggest that the current models of cachectic wasting may oversimplify the complex wasting that occurs in the cancer. Moreover, the pathogenesis of each of these features may be distinct from each other.

1.5 Sarcopenia

The classical definition of cancer-associated cachexia is muscle loss with or without the loss of adipose tissue (20). In some instances, muscle atrophy can occur without fat loss, as is

seen in sarcopenic obese individuals. Sarcopenic obesity has been reported in a number of cancer populations, including CRC and other gastrointestinal cancers, as well as lung cancers. Sarcopenic obesity is associated with particularly poor survival outcomes (35-37). Sarcopenia in association with fat loss is often seen in more aggressive malignancies, such as pancreatic cancers(38). The question is whether phenotype (sarcopenia alone, sarcopenia plus fat loss, or obese sarcopenia) is a product of host susceptibility and premorbid health, or whether the type and biology of the tumor play a role.

There are differences in sarcopenia prevalence in different tumor types. For instance, sarcopenia prevalence is upwards of 80% of patients with gastrointestinal cancers and 50% of patients with colorectal cancers. It is less frequently observed in breast cancers (39). When present, sarcopenia has a number of clinical consequences. In most studies, sarcopenia is associated with reduced overall and disease-free survival (30). Moreover, patients with severe muscle loss have been shown to have reduced tolerance to treatments, such as radiation and chemotherapy (40).

1.5.1 Mechanisms Associated with Sarcopenia Development

There are several well-established mechanisms (and associated circulating mediators) that are related to skeletal muscle wasting in cancer. The most prominent perturbation that results in muscle wasting is a reduction in protein building pathways with a subsequent increase in catabolic processes (23). The development of a net catabolic response is multifactorial but is largely related to inflammation and tumor-mediated factors. In the following section, the topics of discussion will be: systemic inflammation, the acute phase response and a decrease in protein

anabolism with exaggerated catabolic processes, such as proteasomal degradation and autophagy.

1.5.2 Systemic Inflammation

Sarcopenia measurable by CT scan has been shown to be associated with an elevated immune response (41). Tumor-promoting inflammation has emerged as a hallmark of cancer (42). Historically, immune responses were thought to exist solely as an anti-tumorigenic response; however, it is now recognized that the tumor and the associated microenvironment secrete a number of bioactive molecules (i.e. growth factors and pro-inflammatory cytokines) that help promote tumor growth and, perhaps consequentially, induce tumor-mediated muscle wasting (42). IL-6 is one cytokine that can be released from the tumor, and elevated levels of this cytokine is associated muscle proteolysis and atrophy through a STAT3-related mechanism (43).

Not all inflammatory mediators associated with sarcopenia originate from tumor, of course. Elevated levels of IL-6 and C-reactive protein in sarcopenic patients have been described, suggesting that these patients have a more generalized proinflammatory state. (44) (45). Tumor-associated systemic inflammation triggers the release of cytokines into the circulation, several of which are well-established. Two such examples are tumor necrosis factor alpha (TNF-α) and interferon-γ (IFN-γ) (46). TNF-α is released from immune cells, tumor cells and adipocytes and triggers skeletal muscle breakdown by the downstream activation of the NF$\kappa\beta$ pathway, which in turn blocks the activation of the *Myod1* gene, preventing myoblast differentiation (47). IFN-γ works synergistically with TNF-α via a similar mechanism to further promote muscle degradation (48). In addition, TNF-α and IFN-γ also promote muscle proteolysis/autophagy through the

activation of forkhead box protein O (FOXO) related pathways, which upregulate the gene expression of such mechanisms (48).

Another cytokine, IL-1β, has been described to act on the hypothalamic–pituitary–adrenal (HPA) axis and stimulate the production of glucocorticoids (such as cortisol) (49, 50). Cortisol, a catabolic stress hormone, among a myriad of other metabolic effects, also leads to increased muscle wasting by activating the FOXO pathway and blocking IGF-1/PI3K/Akt muscle growth (50). Hypothalamic inflammation related to IL-1β, as well as increased circulation of TNF-α and IL-6, also suppress orexigenic peptides, such as ghrelin and leptin, which further perpetuates tissue wasting (51).

1.5.3 Dysregulated Muscle Maintenance: Decreased Anabolism

Maintenance of skeletal muscle tissue is a fine balance between anabolic (building) and catabolic (breakdown) processes (52). In cancer settings, sarcopenia is related to a dysregulation of skeletal muscle maintenance leading to net elevation of catabolic mechanisms (53). Elevated protein catabolism allows for building blocks required for enhanced tumor growth to be released into circulation (54). Two established mechanisms of catabolic wasting are: decreased growth-factor mediated skeletal muscle growth and decreased myogenic differentiation.

A pathway that promotes skeletal muscle growth is activation of the IGF-1/PI3K/Akt pathway (55). Binding of insulin-like growth factor 1 (IGF-1) and insulin triggers down-stream effects that promote protein anabolism and blocks protein degradation caused by the FOXO family (56). A general decrease in circulating IGF-1 has been documented in cancer likely in association with the onset of the enhanced inflammatory state of the host (57). In addition, the

physical inactivation of IGF-1 through the binding of proteins such as IGFBP3 renders IGF-1 incapable of binding to its receptor and prevents protein synthesis (58, 59). Additionally, muscle synthesis via IGF1/PI3K/Akt has been shown to be inhibited by upregulated circulating cortisol as well as through myostatin, which phosphorylates Akt and inhibits downstream mTOR activity and associated protein synthesis (60). In addition, stress hormones such as cortisol increase resistance to insulin in cancer patients with sarcopenia, further inhibiting muscle growth (60).

Myogenic differentiation is also reduced in tumor-mediated skeletal muscle wasting. TNF-α has been shown to inhibit myoblast differentiation via induction of the NF$\kappa\beta$ pathway (61). Tumor-derived factors, such as myostatin and activin-a inhibit muscle protein synthesis (62). These factors are members of the TGF-beta superfamily and bind to activin receptor type IIB (ActRIIB) receptors to induce muscle wasting through SMAD signaling pathways (60). As mentioned previously, myostatin also inhibits the activation of mTOR pathways and promotes FOXO family activation, enhancing skeletal muscle proteolysis (60).

1.5.4 Dysregulated Muscle Maintenance: A Shift Towards the Catabolic State

Muscle atrophy occurs secondary to activation of catabolic processes in conjunction with the previously mentioned downregulation of anabolic processes. At the cellular level, catabolic processes include: upregulation of ubiquitin-mediated proteasome degradation (UPR) as well as skeletal muscle autophagic mechanisms. These mechanisms can be induced by tumor and host-derived circulating features.

The UPR system is the primary protein degradation mechanism in humans and, when activated, degrades the contractile proteins of skeletal muscle tissue. In cancer-mediated

cachexia, two E3 ubiquitin ligases are activated: muscle-specific RING-finger 1 (MuRF1) and muscle atrophy F-box (MAFBx)/atrogin-1 (63). These E3 ligases tag proteins for proteasomal degradation and have been observed in cancer muscle wasting. The activation of this system has been traced back to TNF-α and myostatin signaling, which activates the FOXO family and upregulates the UPR system through elevated production of E3 ubiquitin ligases (64, 65).

In addition to proteasomal degradation, enhanced autophagic-lysosomal protein degradation is also partly involved in cancer-associated muscle atrophy. Autophagy is a normal part of muscle homeostasis as it helps to eliminate damaged proteins and organelles in skeletal muscle; however, upregulation of this system contributes to enhanced skeletal muscle wasting in cancer settings (46). Similar to what is observed in UPR system activation, activation of FOXO-related mechanisms and can be triggered by glucocorticoid-induced atrophy (i.e. cortisol) as well as IL-6 involvement (66, 67).

1.6 Myosteatosis

Another body composition feature more recently recognized as a consequence of cancer is ectopic lipid accumulation in skeletal muscle, or myosteatosis (68). On CT imaging, myosteatosis appears as low radiodensity skeletal muscle. I have reported that the prevalence of myosteatosis varies in different cancer populations (69). Myosteatosis is associated with diabetes mellitus, obesity and advanced age (70, 71). The clinical impact of myosteatosis also varies with the clinical circumstances, including tumor type. In some studies, myosteatosis is an independent predictor of overall and disease-free survival (72-75). Patients with myosteatosis also reportedly have longer post-surgical lengths of stay in hospital (73).

The main etiologies of myosteatosis in the cancer setting are not well-understood. Systemic inflammation and dysregulated mitochondrial metabolism in the cancer microenvironment have been implicated (76). Metabolic perturbations that lead to mobilization of circulating lipids may also be involved.

1.6.1 Systemic Inflammation

Myosteatosis in the cancer setting has been shown to be associated with systemic inflammation. For instance, a high neutrophil-to-lymphocyte ratio (NLR) (a measure of the presence of systemic inflammation) was found in human patients with pancreatic/CRC cancer in association with myosteatosis (36, 77). Another study of 650 patients with operable CRC demonstrated that low skeletal muscle radiodensity was associated with a higher modified Glasgow Prognostic Scores (mGPS), another measure of systemic inflammation (78). These studies were cross-sectional, therefore causation cannot be determined. However, this work does demonstrate that inflammation is a factor(78).

Outside of the cancer setting, systemic inflammation has also been linked to myosteatosis. For instance, Miljkovic et al. demonstrated that calf muscle radiodensity is inversely correlated with levels of CRP in a cross-sectional study of a healthy Afro-Caribbean cohort (79). High muscle radiodensity has also been associated with reductions in circulating CRP, IL-6 and resistin according to a cross-sectional study done within the Multi-Ethnic Study of Atherosclerosis (MESA) (80). Elevated circulating inflammatory markers may be largely related to central obesity, as high abdominal intramuscular adipose tissue surface area is associated with increased CRP, IL-6 and leptin (81).

Circulating mediators related to systemic inflammatory processes, such as TNF-α and IL-6, have been shown to promote lipolysis in white adipose tissue (82). Enhanced lipolysis, both derived from inflammatory/metabolic mediators as well as dysfunctional adipocyte storage in obesity, result in an elevation of circulating lipids. An excess in circulating lipids increases the likelihood that fat is ectopically placed in depots such as the liver or skeletal muscle tissue, known as lipotoxicity (83). Excess lipid accumulation in skeletal muscle tissue can cause disruptions of normal glucose metabolism and influence insulin sensitivity in muscle tissue, which is a major site of glucose disposal in healthy settings (84).

1.6.2 Metabolic Perturbations

States of systemic inflammation, such as in obesity, have been shown to cause changes to normal metabolic processes. One such mechanism is related to the onset of elevated lipids in circulation as a result of enhanced lipolysis. For instance, myosteatosis is commonly observed in individuals with insulin resistance and a further understanding of this mechanism may provide insight into cancer-associated lipid accumulation in muscle (85). Increases in circulating lipids can lead to ectopic accumulation in skeletal muscle tissue. Specifically, excess free fatty acids in muscle are converted to acetyl-CoA which eventually leads to diacylglycerol (DAG) and triacylglycerol (TAG) production (84). TAGs are stored in cells as lipid droplets, which cause an overall decrease muscle radiodensity (84). Interestingly, DAGs can activate protein kinase C which blocks insulin receptor tyrosine kinase (IRTK) inhibiting downstream activity of the PI3K/Akt pathway which may inhibit normal muscle growth mechanisms (84).

It has also been postulated that dysfunctional mitochondria can induce lipid accumulation in skeletal muscle tissue. For instance, RNA-sequencing of muscle biopsies from pancreatic cancer patients with myosteatosis demonstrated features consistent with reduced lipid oxidation (32). Declines in lipid oxidation may induce the collection of lipid droplets observed in muscle. Wilson et al. similarly demonstrated that myotubes exposed to breast cancer conditioned media developed mitochondrial dysfunction that triggered intracellular lipid deposition in these cells (76). It was hypothesized that the mechanism of myotube lipid accumulation was related to reduced peroxisome proliferator-activated receptor (PPAR) activity, which is responsible for the transport and oxidation of fatty acids (76).

1.7 Dense Subcutaneous Adipose Tissue

In recent years, there is increasing attention on the influence of adipose tissue radiodensity on cancer outcomes. Specifically, adipose tissue density in the subcutaneous region has been shown to decrease overall survival outcomes in cancer types such as colorectal cancer and esophageal cancer (33, 34, 86). There is limited work that has been completed that describes what mechanisms may be responsible for the development of dense sub-q. It has been postulated that decreases in adipocyte size, adipocyte browning (that occurs with cancer cachexia) and inflammation may be to blame (33).

1.7.1 Adipocyte Wasting

The primary function of white adipose tissue (WAT), which is observable in the subcutaneous region, is to synthesize and store triacylglycerol (TAG) (87). In times of energy deprivation (or in metabolically demanding states such as cancer cachexia), lipolysis is enhanced,

and free fatty acids/glycerol are released into circulation for energy utilization elsewhere (87). As previously described, systemic inflammation has been shown to be increased in cancer cachexia, and pro-inflammatory circulating factors, such as TNF-α and IL-6 are linked to the promotion of enhanced lipolysis in the cachexia setting (23). With these mechanisms in mind, it has been proposed that an increase in fat radiodensity may be related to adipocyte size, specifically with a reduction in lipid content (increasing radiodensity within the CT scan) (33).

1.7.2 Adipose Tissue Browning

Another potential mechanism that may be involved in the detection of dense adipose tissue is a mechanism involved in cancer cachexia, which is the browning of adipose tissue. The conversion of WAT to brown adipose tissue (BAT) has been described in mouse models of lung and pancreatic cancers (88). Specifically, adipose tissue browning involves an increase in mitochondrial content within adipocytes and a metabolic shift to enhanced energy expenditure (related to increased uncoupling activity via uncoupling protein 1) (88). This increase in energy expenditure is a reflection of enhanced lipid utilization. The transition of WAT to BAT is related to increased circulating IL-6, which can be derived from tumors, and promotes adipose tissue browning potentially through the recruitment of macrophages or B-adrenergic activation (88). Tumors that have elevated secretion of parathyroid hormone-related protein (PTHrP) have also been shown to enhance the conversion of WAT to BAT in cancer cachexia (89). The transition of healthy WAT to BAT in the subcutaneous region may be related to the increased density of adipose tissue detected in some patients with cancer.

1.8 Study Rationale

1.8.1 Models of Cancer Wasting do Not Account for Diverse Body Composition Phenotypes

As was previously discussed, there are several body composition phenotypes that are observable in cancer populations. At present, sarcopenia is currently the only abnormal body composition phenotype that is well-described under tumor-mediated models of wasting. BC phenotypes such as myosteatosis or highly dense adipose tissue are not included within classical models of cancer cachexia. However, the abundance of evidence demonstrating that additional BC phenotypes exist beyond muscle wasting in cancer populations that worsen patient outcomes highlights that tumor-mediated tissue wasting models require further supplementation. Indeed, the classical models of cancer cachexia are currently not sufficiently inclusive or descriptive to explain other BC phenotypes, such as myosteatosis and highly dense adipose tissue.

In colorectal cancer (CRC), there is previous literature to demonstrate that sarcopenia, myosteatosis and dense sub-q are observable in this cancer type. However, there is limited literature that examines the co-existence of these phenotypes and the influence of each on survival outcomes. Furthermore, there is limited knowledge of any biological correlates of proteins related to cachectic wasting in relation to each BC phenotype, especially with regards to myosteatosis and dense sub-q.

The objective of this study is to determine the prevalence and influence of sarcopenia, myosteatosis and dense sub-q BC phenotypes in a cohort of patients with colorectal cancer (stages I – IV). I would like to gain a better understanding of the co-relationships of various body composition features .I am also interested in evaluating proteomic features in circulating sera

and as well as the tumor proteome in relation to body composition features detected in the cohort.

1.8.2 Hypothesis

I hypothesize that colorectal tumors would drive changes in body composition beyond muscle wasting, manifesting as myosteatosis and dense sub-q (in addition to sarcopenia). I also postulate that each body composition phenotype is associated with its own respective proteomic markers (in the blood as well as in the tumor).

1.8.3 Specific Aims

This project has three specific aims. Aim 1 is to determine the incidence, co-relationship and clinical consequence of sarcopenia, myosteatosis and dense sub-q body composition features in pre-operative CT images from patients with colorectal adenocarcinoma (stages I – IV) (Chapter 3). Aim 2 is to evaluate targeted, circulating proteins in serum samples in relation to the three body composition features evaluated in Aim 1 (Chapter 4). In Aim 3, label-free shotgun proteomics will be conducted on colorectal adenocarcinoma tumor samples in relation to body composition features identified in Aim 1.

Chapter 2: Materials and Methods

2.1 Body Composition Analysis (Aim 1)

2.1.1 Cohort Selection

This study was approved by the Health Research Ethics Board of Alberta (HREBA.CC-16-0959; HREBA.CC-19-0043; HREBA.CC-16-0485_REN2). The primary population under assessment in this project was a cohort of 319 patients with colorectal adenocarcinoma (stages I – IV) who underwent surgical resection in Calgary, Alberta and who had available preoperative CT cans. This population represented the "discovery" cohort. An external validation consisted of a cohort of patients with CRC from Edmonton, AB (N = 960). CT scans were analyzed by a different technician at the University of Alberta (72).

All patients from the Calgary cohort provided consent, as blood samples and tumor samples were collected in parallel as part of a prospective study. For the discovery cohort, DICOM imaging files from CT scans were obtained from the Calgary Image Processing and Analysis Centre at the Foothills Medical Centre, Calgary, Alberta.

The validation cohort consisted of 960 patients with stage I – III CRC, all of which had a pre-operative CT image. These patients underwent surgical resection with curative intent between 2007 and 2009. The Health Research Ethics Board of Alberta at the University of Alberta approved this study and any additional cohort characteristics have been previously described (72). Detailed population characteristics of the discovery and validation cohorts can be observed in Table 2.1 below. The Edmonton study was retrospective, and so consent was waived.

Variable		Discovery cohort (n = 319)	Validation cohort (n = 960)
Age	Years	64.2 ± 12.5	65.8 ± 11.8 years
Sex	Females Males	138 (56.7) 181 (43.3)	378 (60.6%) 582 (39.4%)
Overall Stage	Stage 1 Stage 2 Stage 3 Stage 4	65 (20.4) 84 (26.3) 97 (30.4) 73 (22.9)	99 (10.3%) 371 (38.6%) 490 (51.0%) 0 (0%)
Diabetic status	Non-diabetic Diabetic	264 (82.8) 55 (17.2)	NA NA
Sarcopenia status	No sarcopenia Sarcopenia	184 (57.7) 118 (37.0) Missing: 17	478 (49.8%) 482 (50.2%)
Myosteatosis status	No myosteatosis Myosteatosis	233 (73.0) 86 (27.0)	599 (62.4%) 361 (37.6%)
Dense sub-q status	No dense sub-q Dense sub-q	279 (87.5) 40 (12.5)	831 (86.6%) 129 (13.4%)

Table 2.1. Patient characteristics in the discovery and validation cohorts.

2.1.2 Image Selection and Radiographic Measurements

Radiographic measurements were completed to assess skeletal muscle and adipose tissue surface area and radiodensity (N = 319). Specifically, a pre-operative, axial CT image was extracted at the level of the third lumbar vertebra (L3) for each participant. This slice was selected because L3 is commonly utilized in the literature, since it provides the best correlate for whole-body skeletal muscle and adipose tissue volume (90). The image was analyzed with Slice-O-Matic software (v.5.0, Tomovision, Montreal, Canada). This software quantifies the surface area of muscle and adipose tissue in cm^2 in addition to the radiodensity of the pixels within the CT image on the Hounsfield Unit (HU) scaling system. The HU scaling system quantifies relative radiodensity of tissues within CT images and is standardized to water (0 HU) and air (−1000 HU) (28). Soft tissues were evaluated at previously validated radiodensity thresholds: skeletal muscle

included tissues with a radiodensity of −29 to +150 HU, inter-muscular adipose tissue and subcutaneous adipose tissue were evaluated at radiodensity thresholds of -190 to -30 HU and visceral adipose tissue was evaluated at radiodensity thresholds of -150 to -50 HU (28).

2.1.3 Phenotype Definitions

Three specific body composition phenotypes were evaluated in both the discovery and validation cohorts: sarcopenia, myosteatosis and dense subcutaneous adipose tissue (dense sub-q). Sarcopenia (low muscle mass) was defined by using previously validated cut-points by Martin et al. (91). These values use skeletal muscle index (SMI) cut-offs to dichotomize into sarcopenic and non-sarcopenic groups. SMI is calculated by dividing skeletal muscle surface area in cm^2 by height in m^2, which standardizes for patient size. Martin sarcopenia definitions are dependent on sex and body mass index (BMI) and sarcopenia in men is defined as SMI's < 43 cm^2/m^2 for BMI's < 24.9 and SMI's < 53 cm^2/m^2 for BMI's ≥ 25. Sarcopenia is defined as SMI < 41 cm^2/m^2 in women in all BMI categories. There were 20 male patients of which BMI status was missing, and in those cases the Fearon definitions of sarcopenia were utilized (20). Myosteatosis was defined by a previously validated cut-point of 30 HU (32). Dense subcutaneous adipose tissue is new to the literature and no validated cut-points currently exist for this phenotype; therefore, we defined a cut-point specific to this population using the R Studio package, Evaluate Cutpoints (92). The *maxstat* function was utilized which finds a value on a continuous scale that most significantly splits the cohort, via optimized stratification, into better and worse overall survival outcomes based on a standardized log-rank test. The resulting cut-point was -87 HU.

2.2 Targeted Proteomic Analysis (Aim 2)

2.2.1 Study Cohort

Using the discovery set, 119 of CRCs (stages I – IV) were included for analysis. These patients all had pre-operative CT images as well as associated pre-operative serum samples obtained within 100 days of the CT scan. Any of the remaining 319 patients did not have pre-operative serum and were excluded from this aim.

2.2.2 Protein Selection

Twenty proteins were selected for targeted proteomic analysis. These proteins had diverse functions, including: inflammatory processes, involvement in energy homeostasis and muscle maintenance. These proteins were chosen to give a well-rounded view of commonly described phenomenon within cachexia wasting models. Protein selection can be observed below:

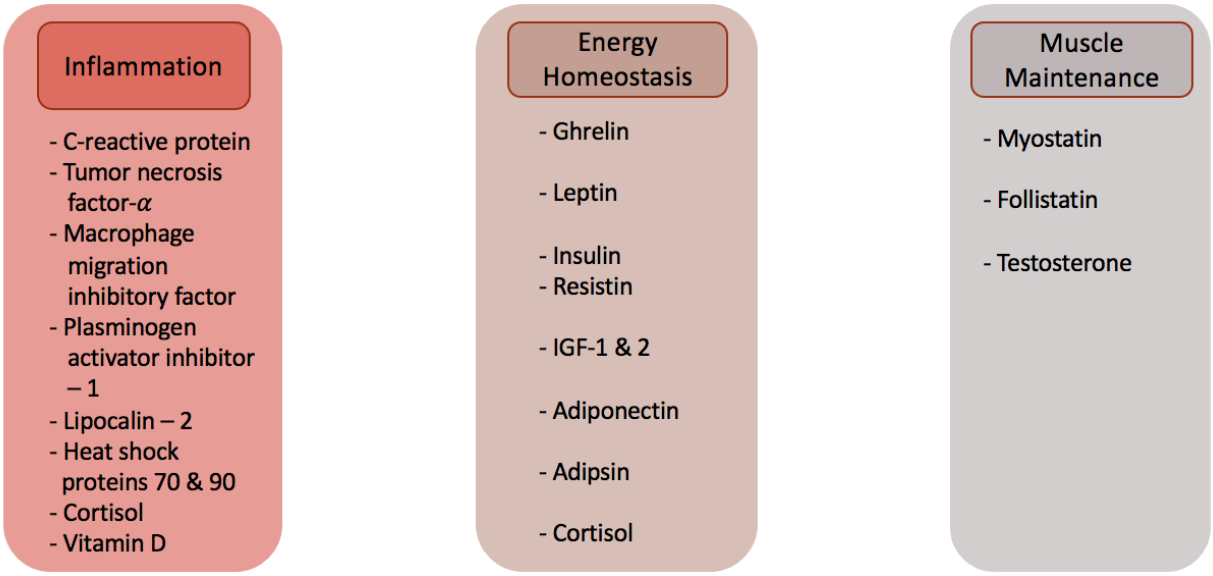

Figure 2.1 Overview of proteins selected for targeted proteomics.

Table 2.2 below provides a further description of the function of these proteins (same order as above).

C-Reactive Protein (CRP)	An acute phase protein commonly used as a marker of systemic inflammation, and regarded as an indicator of cancer-associated wasting disorders (93).
Tumor Necrosis Factor-Alpha (TNF-a)	Well-documented, pro- inflammatory and cachexic marker responsible for several pathological mechanisms such as: skeletal muscle proteolysis, lipolysis and increased gluconeogenesis (94).
Macrophage Migration Inhibitory Factor (MIF)	Pro-inflammatory cytokine involved in the proliferation and increased invasiveness of the tumor (95).
Plasminogen Activator Inhibitor-1 (PAI-1)	Pro-angiogenic and protective influence on several cancer types; promotes the recruitment of tumor-associated macrophages, proinflammatory phenotype (96).
Lipocalin-2	An adipokine that has been associated with increasing skeletal muscle regeneration and activation of skeletal muscle satellite cell recovery (97).
Resistin	The role of resistin in metabolic dysregulations, such as within cancer, are not completely understood. However, some research suggests that it is related to obesity, type II diabetes and increased visceral fat. In addition, it is hypothesized to play a role in the inflammatory state (98).
Heat Shock Proteins 70 & 90 (HSP 70/90)	Cancer-associated release factors that act in the development/progression of muscle wasting via the ubiquitin-proteasome and autophagy-lysosome pathways (99).
Cortisol	Cortisol, released from adrenal glands and stimulated from other inflammatory cytokines such as CRP and TNF-alpha, plays a role in elevated systemic inflammation in patients with cancer. Elevated cortisol is thought to enhance protein degradation in cachexia by enhancing the ubiquitin-proteasome system. Is also thought to enhance lipolysis and beta-oxidation (100).
Vitamin-D	Vitamin-D deficiency is commonly observed world-wide, and is associated with cancer. Administration of vitamin-D in patients with cancer, to ameliorate conditions such as cachexia, is contradictory in the literature. Is hypothesized to delay onset of sarcopenia, although research is limited (101).
Ghrelin	Powerful inducer of growth hormone; stimulates food intake and adiposity (102). Is expected to correlate positively with cachectic states.
Leptin	Adipocytokine that induces satiety and stimulates energy expenditure (103). Leptin levels have been associated as lower in patients with cachexia.
Insulin, IGF-1 & IGF-2 System	Overall, plays an important roles in tissue growth and development. For ubiquitin-proteasome system seems to be importantly involved in cachectic muscle wasting; overexpression related to cachexia as IGF-1 and insulin suppress expression of this pathway; theoretically, reduced IGF-1 and insulin expression are related to increase protein degradation via this system.

	Insulin-resistance is also associated with a reduction of signals that induce protein synthesis and inhibit protein breakdown (104).
Adiponectin	Secreted exclusively from adipose tissue; stimulates fatty acid oxidation in skeletal muscle and inhibits gluconeogenesis[40]. Low circulating levels of adiponectin is associated with insulin resistance, type II diabetes and obesity (105).
Adipsin	Correlates positively with increased adiposity. It is hypothesized that the adipsin-acylation stimulating protein system plays a role in the clearance of circulating triacylglycerol from plasma (39). This factor is also thought to stimulate triglyceride synthesis in adipose tissue (106).
Myostatin	A member of the TGFβ family, enhanced expression is associated with muscle atrophy. Demonstrated to increase in response to inflammatory signalling (107).
Follistatin	Potent inhibitor of myostatin, commonly observed in exercised states, promoting muscle growth (108).
Testosterone	Decreased circulating testosterone concentrations are associated with loss of lean muscle mass, particularly in male cancer patients. Preliminary data suggest that supplementation with exogenous testosterone can increase skeletal muscle mass in male and female patients (109).

Table 2.2. Proteins included in the targeted proteomic analysis and their functional significance.

2.2.3 Serum Analyses

Pre-operative sera from patients with preoperative CT scans (N= 116) were utilized for targeted proteomic analysis using multiplexed protein bead assays (Eve Technologies, Calgary, AB). Blood samples were collected in red top Vacutainers (Becton Dickinson) then centrifuged. Serum was separated and stored in a –80 freezer. Selected serum samples were submitted for multiplexed LASER bead assay analysis. Briefly, multiplexed LASER bead technologies use polystyrene beads colored by red and infrared fluorophore dyes that uniquely bind specific analytes and produce specific colors based on the identity of the analyte (110). A bead analyzer

(Bio-Plex 200) is then used to quantify analyte concentrations when compared to a standard curve in a dual-laser/flow-cytometry system (110).

2.3 Untargeted Tissue Proteomics – Aim 3

2.3.1 Sample Selection

A total of 65 pre-operative patient scans (within 90 days of surgery) were completed that had associated tumor samples from Dr. Oliver Bathe's biobank. Based on sample availability and body composition phenotype, tumor samples were selected; they had either sarcopenia alone, myosteatosis alone, or neither. Dense sub-q was not included, as there were insufficient samples. For consistency in the cut-points for sample selection, the lower tertile of the continuous body composition measurements from the discovery cohort (n = 319) were used to define sarcopenia and myosteatosis. Unfortunately, there were not enough females who met these criteria and therefore only male samples were utilized. A total of 14 patients were included in this analysis. These patients were treatment naïve and underwent surgical resection. The cohort overview for this aim is summarized in Table 2.1.

Body Composition	N	Age	Sex	Overall Stage	SMRD (HU)	SMI ($\frac{cm^2}{m^2}$)	Sub-Q density (HU)
Myosteatosis	**4**	70.0 ± 10.3	0 (0%) F 4 (100%) M	Stage 1: 0 Stage 2: 1 Stage 3: 2 **One N/A**	27.5 ± 1.7	58.0 ± 6.4	-101.2 ± 1.9
Sarcopenia	**5**	69.2 ± 7.6	0 (0%) F 5 (100%) M	Stage 1: 1 Stage 2: 3 Stage 3: 1	39.3 ± 5.8	46.1 ± 2.0	-94.7 ± 6.8
No Features	**5**	61.6 ± 9.6	0 (0%) F 6 (100%) M	Stage 1: 2 Stage 2: 1 Stage 3: 2	44.9 ± 7.4	62.4 ± 7.0	-97.7 ± 5.1

Table 2.3. Label-free untargeted proteomics - cohort overview.

2.3.2 Sample Preparation and Liquid Chromatography–Tandem Mass Spectrometry

The CRC tumor tissues were embedded in optimal cutting temperature compound (OCT compound) and stored at –80°C. Five sections from each sample block were cut at thicknesses of 8 μm. One section was stained with hematoxylin and eosin for pathological examination to ensure adequate tumor content.

Unstained sections were included for the label-free proteomics analysis. Briefly, each tumor sample was subjected to an independent acetone precipitation of proteins to remove undesirable substances that interfere with downstream analysis. After the acetone precipitation, the protein pellets were individually resuspended in a solution of urea 8M in 100mM of tris-HCL (pH 8), which also aided in removing remaining acetone as well as OCT. The reducing agent dithiothreitol (1M) was added to each sample to eliminate disulfide bonds to aid in linearizing protein chains. Each independent sample was then moved to Microcon-30kDa centrifugal filter units (MRCF0R030) and each were washed with urea-tris for removal of unwanted residues such as OCT, lipids, DNA and additional desalting. A wash with iodoacetamide (50mM) was then conducted to inhibit cysteine residue refolding. After 3 additional washes with Urea-Tris, an ammonium bicarbonate (50mM) wash was then performed to remove any remaining urea-tris. A trypsin digestion (Promega MS grade; PRV5111) was then completed overnight at 37°C. Finally, digested samples were subjected to Pierce™ Peptide Desalting Spin Columns (89851 & 89852) as a final washing step to remove the ammonium bicarbonate, remaining SDS detergent and salts.

The desalted peptides from each sample (eluted with 0.1% TFA, 50% ACN) were resuspended in 0.1% formic acid and were then ready for LC-MS/MS analysis (N = 14).

Prepared samples were then submitted for liquid chromatography–tandem mass spectrometry (LC-MS/MS) at the Southern Alberta Mass Spectrometry Facility and the University of Calgary Cumming School of Medicine. The LC-MS/MS instrument utilized was an Orbitrap Fusion Tribrid Mass Spectrometer (Thermo Fisher Scientific).

2.4 Data Analysis – Aim 1

2.4.1 Clinical Data Analysis

Patients were allocated to different groups depending on body composition status, and overlap of phenotypes were documented. For patients with independent body composition features (i.e. independent sarcopenia, myosteatosis, dense sub-q and no features) descriptive group statistics were completed utilizing t-tests for continuous data and Chi-square/Fisher's exact tests for categorical information. This was completed for the available clinical information on the discovery cohort which included: age, sex, T stage, N stage and M stage, and diabetic status. Univariate and multivariate associations of these clinical features, in addition to the previously described body composition phenotypes, and their relevance with overall survival outcomes were explored using cox (proportional hazards) regression analysis in IBM SPSS Version 25.

2.4.2 Survival as a Function of Body Composition Features

To determine whether the body composition phenotypes identified were relevant to overall survival outcomes in this cohort, log-rank statistics were applied. The influence of independent phenotypes on OS were assessed as well as any summative effects when multiple features coexisted. IBM SPSS Version 25 and Prism 9.1.0 were used for statistical analysis and figure generation.

2.4.3 Correlation Analysis – Body Composition

Non-parametric, Spearman rho correlations of the continuous body composition outputs from Slice-O-Matic were performed. This included information on skeletal muscle, intermuscular adipose tissue, and subcutaneous/visceral adipose tissue surface areas and radiodensities. These correlations were performed in R Studio version 3.6.3. Correlation matrices were also generated in R Studio version 3.6.3.

2.4.4 Validation on External Dataset

In order to assess the external validity of the results from the workflow described above, a validation cohort was utilized (72). Specifically, this cohort included 960 patients with colorectal cancer (stages I – III). Cohort characteristics from this validation set can be observed in Table 1 above. The same workflow previously described was performed on this external dataset to validate the discovery set findings. The only additional analysis that was conducted on the validation cohort that wasn't completed on the discovery cohort was the assessment of the prevalence of each body composition phenotype in relation to BMI status.

2.5 Data Analysis - Aim 2 – Targeted Proteins from Multiplex Bead Assay

Comparison of analyte concentrations between the body composition features of interest were completed. First, the analyte concentrations of analytes quantified by multiplexed protein bead assays were compared in patients with a single feature (sarcopenia, myosteatosis or dense sub-q). Significance of any differences was tested using the Kruskal-Wallis one-way analysis of variance test. As a separate posthoc analysis in cases where the Kruskal-Wallis test was significant, Mann-Whitney U tests for patients with sarcopenia vs no sarcopenia, myosteatosis vs no myosteatosis and dense sub-q vs no dense sub-q were also completed. The influence of BMI status was also tested in a posthoc fashion using Mann-Whitney U testing. Finally, non-parametric Spearman's rho correlations were completed for protein concentrations compared to continuous body composition measurements dichotomized by patient sex. All tests of significance were two-sided and p-values of < 0.05 were considered statistically significant. Each test statistic was corrected for multiple comparisons through the Bonferroni correction method. Statistics and graphs were completed in IBM SPSS Version 25, Prism 9.1.0 and R Studio version 1.3.1093.

2.6 Data Analysis – Aim 3 – Untargeted Tissue Proteomics

2.6.1 Bioconductor Package: DEP

Raw spectral mass spectrometry data were processed and quantified in the proteomics software MaxQuant (v2.1.0.0). Differential abundance analyses of proteins from MaxQuant between the sarcopenia and myosteatosis phenotypes compared to patients with no features were completed in the Bioconductor package "DEP" (version 3.15) in the R environment (version 1.3.1093). Data for sarcopenia vs. normal and myosteatosis vs. normal were normalized and

analyzed separately. Briefly, the data from MaxQuant was loaded into the DEP package and a summarized experiment was created. As missing values are a common issue in proteomics experiments, a filtering threshold of 1 was used (i.e. filter for proteins that are identified in 2 out of 3 replicates of at least one condition). Data was then normalized by variance stabilizing transformation and an imputation method for missing values was chosen based on the nature of the missing values. Differential abundance analysis was completed for Sarcopenia vs Normal and Myosteatosis vs. Normal using protein-wise linear models combined with empirical Bayes statistics. Differentially abundant proteins with a $\log_2(2) = 1$ fold change between groups with associated p-values < 0.05 (adjusted for multiple comparisons) were considered significantly different in abundance and used for pathway research (associated volcano plots and heatmaps were generated in via the DEP package).

2.6.2 Targeted and Untargeted Tumor Proteomic Multivariate Assessment - SIMCA-P+ Software

To examine if the phenotypes of interest could be separated based on differences in protein abundance, multivariate Partial Least Squares Discriminant Analysis (PLS-DA) was performed (in both Aims 2 and 3). To identify potential outlier samples and flag any abnormalities in the data structures, a principal component analysis (PCA) was conducted. A subsequent supervised PLS-DA analysis was then performed. Proteins were selected based on variable importance on projection (VIP) thresholds set to maximize R^2Y and Q^2Y values and to minimize the difference between them.

2.6.3 Pathway Analyses

The UniProt Knowledgebase was utilized for the assessment of functional protein information based on the above findings (111). In addition, existing literature on the differentially abundant proteins identified using the DEP package was then described.

Chapter 3: Evaluating Body Composition Features in Colorectal Adenocarcinoma

3.1 Introduction

Tumor-mediated tissue wasting, or cachexia, is frequently observed in patients with CRC. These wasting processes are linked to the growth/progression of the tumor, and cause a net negative energy balance that leads to the wasting of skeletal muscle (and often adipose tissue) (20). The diagnosis of cachexia requires the detection of sarcopenia (low muscle mass) that can be captured through the use of CT imaging techniques. Interestingly, CT assessment techniques have since revealed that additional body composition phenotypes are detectable in CRC, such as lipid accumulation in muscle, or myosteatosis. Specifically, a large body of research has consistently shown that sarcopenia and myosteatosis negatively influence overall survival and disease-free survival in patients with colorectal cancer (72-74). In addition, these body composition phenotypes result in longer hospital stays as well as a higher frequency of postoperative complications (73, 75, 112).

In addition to sarcopenia and myosteatosis, a newly described body composition phenotype that can also manifest in CRC is high density subcutaneous adipose tissue (dense sub-q). This phenotype has also been associated with increased risk of mortality in patients with CRC, and continues to be more frequently recognized as an influential wasting phenotype in the cancer setting (33). Indeed, there is increasing evidence to suggest that tumor-mediated tissue wasting can manifest as different perturbations in body composition beyond just the wasting of muscle. However, prevalence of these three body compositions and the co-existence of each in CRC remains to be elucidated.

Given findings from previous research, we postulated that the classical definition of cancer-associated tissue wasting (cachexia) does not encompass all of the body composition phenotypes that may arise in CRC (75). We hypothesized that colorectal tumors drive changes in body composition beyond muscle wasting and that multiple clinically significant phenotypes exist. Specifically, we were interested in investigating sarcopenia, myosteatosis and dense subcutaneous adipose tissue in our cohort of patients with CRC. We postulated that these phenotypes (measurable via CT scan) would occur independently of one another and would be influential on overall survival outcomes. The first aim of this project is described in this chapter.

3.2 Results Part 1: Discovery Cohort

3.2.1 Sarcopenia, Myosteatosis and Dense Subcutaneous Adipose Tissue are Independent Phenotypes

The discovery cohort consisted of 319 patients with colorectal adenocarcinoma (stages I – IV) and with preoperative CT images. Within that cohort, height was available for SMI calculation in 302 patients. Of these 302 patients, 118 (39%) exhibited the sarcopenia phenotype. From the full 319 cohort, 86 (27%) and 40 (13%) exhibited the myosteatosis and dense subcutaneous fat phenotypes, respectively. When evaluating the 302 patients where sarcopenia, myosteatosis and dense subcutaneous adiposity information were available for each, only one of these features was apparent in 74% (Figure 3.1). The concurrence of all three phenotypes was particularly rare, with only 8 (4%) individuals within the cohort exhibiting them all. Similarly, the overlap of just myosteatosis and dense subcutaneous adipose tissue was almost non-existent,

with only 3 individuals of the 302 patient cohort having both concurrently. Sarcopenia and myosteatosis, the most common combination of features, coexisted in 15%.

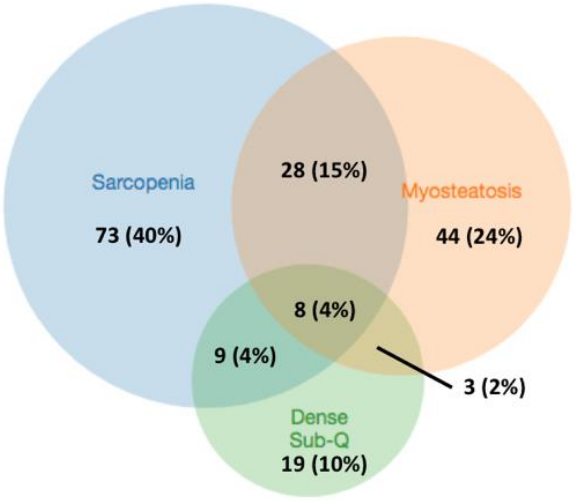

Figure 3.1. Venn diagram displaying phenotypic independence and overlap in the discovery cohort (N = 319). Features display a large degree of independence (74%).

3.2.2 Clinical Characteristic Differences in the Isolated Phenotypes

When we evaluated clinical characteristics in patients with each of the three body composition features (alone), only a few significant differences were detected. Specifically, patients with myosteatosis alone were significantly older (69.3 $\pm$ 9.9 years) than patients who had no "abnormal" body composition features (60.9 $\pm$ 11.8 years) ($P < 0.001$). Additionally, more males had no perturbed body composition features (65.3%) compared to females (34.7%) whereas a higher proportion of females (59.1%) had myosteatosis than males (40.9%) ($P = 0.005$). All relationships between clinical characteristics and body composition features are summarized in Table 3.1.

Variable		No features (NF) N = 118	Isolated sarcopenia (IS) N = 73	P-value NF vs IS	Isolated myosteatosis (IM) N = 43	P-value NF vs IM	Isolated dense sub-q (ID) N = 19	P-value NF vs ID
Age	--	60.9 ±11.8 yrs	63.9 ± 12.9 yrs	0.101	69.3 ± 9.9	< 0.001	59.3 ± 15.5	0.594
Sex	Females Males	41 (34.7) 77 (65.3)	34 (46.6) 39 (53.4)	0.104	26 (59.1) 18 (40.9)	0.005	8 (42.1) 11 (57.9)	0.535
T stage	Stage 1 Stage 2 Stage 3 Stage 4	13 (11.2) 18 (15.5) 60 (51.7) 25 (21.6) Missing: 2	11 (15.1) 13 (17.8) 31 (42.5) 18 (24.7)	0.647	3 (7.1) 6 (14.3) 26 (61.9) 7 (16.7) Missing: 2	0.686	0 (0) 2 (10.5) 13 (68.4) 4 (21.1)	0.355
N stage	Stage 0 Stage 1 Stage 2	50 (42.4) 37 (31.4) 31 (26.3)	39 (54.9) 21 (29.6) 11 (15.5) Missing: 2	0.146	24 (55.8) 12 (27.9) 7 (16.3) Missing: 1	0.260	6 (31.6) 9 (47.4) 3 (21.1)	0.389
M stage	No metastasis Metastatic	91 (79.8) 23 (20.2) Missing: 4	51 (69.9) 22 (30.1)	0.120	38 (88.4) 5 (11.6) Missing: 1	0.212	13 (68.4) 6 (31.6)	0.265
Diabetic status	No diabetes Diabetes	99 (83.9) 19 (16.1)	65 (89.0) 8 (11.0)	0.322	33 (75.0) 11 (25.0)	0.195	17 (89.5) 2 (10.5)	0.531

Table 3.1. Clinical characteristics in patients with isolated phenotypes (sarcopenia, myosteatosis or isolated dense sub-q, alone) compared to patients exhibiting no "abnormal" body composition phenotypes, discovery cohort.

3.2.3 Myosteatosis and Dense Subcutaneous Adipose Tissue are Independent Predictors of OS

To determine the influence of each of the body composition phenotypes on the overall survival in the discovery cohort (n = 319) univariate and multivariate cox regressions were performed. Myosteatosis and dense subcutaneous adipose tissue were both observed to be independent predictors of overall survival outcomes even when N stage and metastatic disease were taken into consideration ($p < 0.001$, $p = 0.050$, respectively) (Table 3.2). Sarcopenia as defined by the criteria from Martin et al (ref) was not associated with a reduction in survival ($p = 0.414$).

PARAMETER	COMPARISON	UNIVARIATE ANALYSIS		MULTIVARIATE ANALYSIS	
		HR	*P*-value	HR	*P*-value
AGE	--	1.013	0.199		
SEX	Male vs. Female	1.224	0.379		
T-STAGE	1 vs 2 1 vs 3 1 vs 4	2.411 8.637 14.32	0.431 0.033 0.009	1.458 3.574 4.263	0.738 0.213 0.164
N-STAGE	0 vs 1 0 vs 2	3.245 4.643	< 0.001 < 0.001	2.696 3.644	0.002 < 0.001
METASTASIS	M0 vs. M1	2.673	< 0.001	1.791	0.032
DIABETES	NO vs. YES	1.267	0.391		
MYOSTEATOSIS	NO vs. YES	1.696	0.025	2.617	< 0.001
SARCOPENIA	NO vs. YES	1.206	0.414		
HIGH RADIODENSITY	Low vs. High	2.164	0.006	1.772	0.050

Table 3.2 Univariate and multivariate cox regression of clinical features and body composition phenotypes.

Interestingly, when all phenotypic overlap was removed, sarcopenia became statistically significant at reducing overall survival compared to patients with no body composition phenotypes (p = 0.002). Isolated myosteatosis and dense sub-q remained statistically significant on survival outcomes (Figure 3.2).

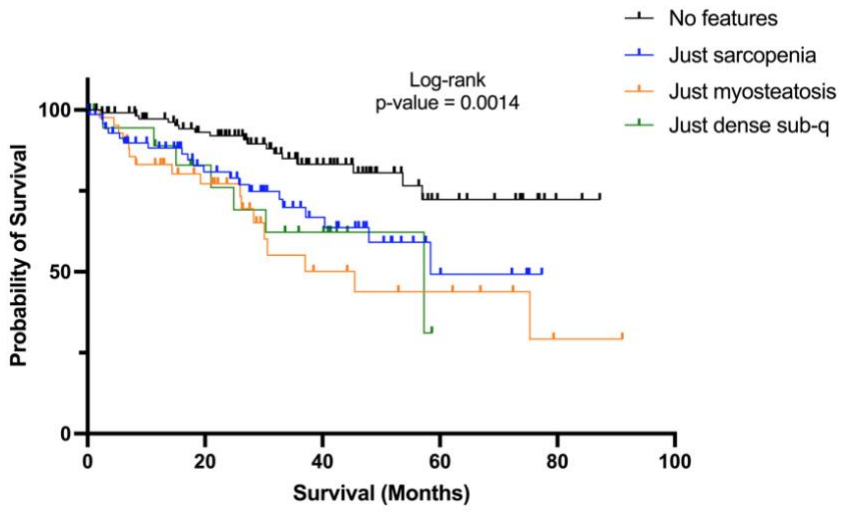

Figure 3.2. Independent phenotypic influences on OS. Kaplan-Meier survival analyses revealed isolated phenotypes reduce lengths of OS when compared to patients with no features (P = 0.002).

3.4.3 Phenotype Overlap Influences Survival Outcomes

Consistently, patients with no abnormal body composition features had the best overall survival outcomes in both the independent and summative assessments (Figures 3.2 & 3.3). The impact of overlapping phenotypes on survival outcomes also produced significant findings. Specifically, the concurrence of all three phenotypes was associated with particularly poor overall survival outcomes ($p < 0.001$) (Figure 3.3).

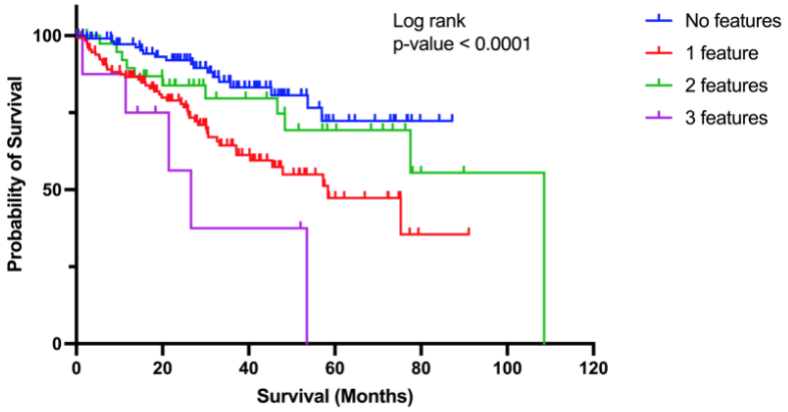

Figure 3.3. Evaluation of phenotypic overlap on OS. Kaplan-Meier survival analyses revealed that the overlap of three body composition phenotypes is particularly detrimental to OS (P < 0.001).

3.4.5 Correlations of Continuous Body Composition Data

Spearman rho correlations revealed that several of the continuous body composition measurements (when dichotomization into groups was removed) have strong and significant associations (Figure 3.4). One correlation of particular interest is that of SAT surface area and SAT radiodensity. There is a curvilinear relationship between the two, where lower SAT surface area is associated with higher radiodensity values ($r = -0.59$, $P < 0.001$). Specifically at around 150 cm^2 there is a particularly sharp elevation in radiodensity.

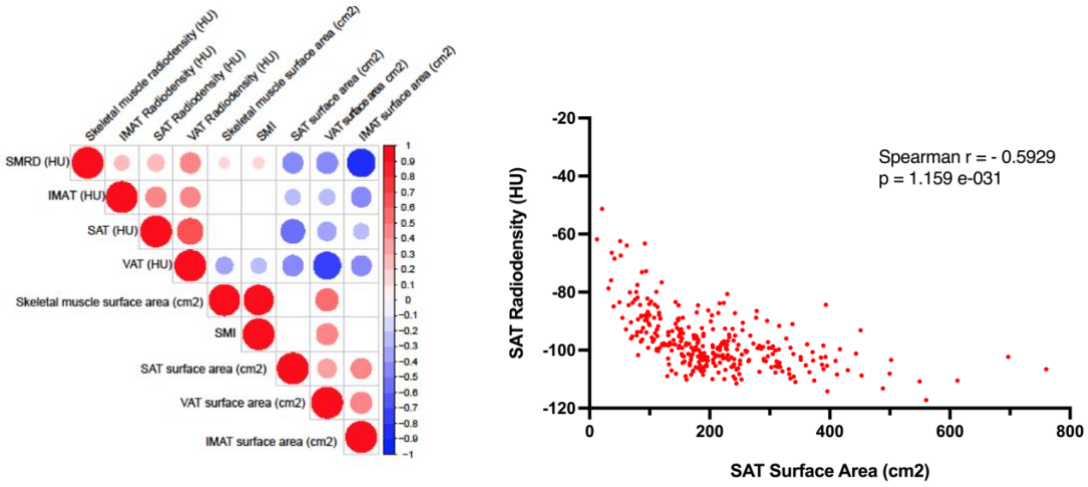

Figure 3.4. Correlation matrix of continuous body composition measurements. Spearman rho correlations of continuous body composition values revealed a strong, negative correlation of SAT surface area (cm^2) and SAT radiodensity, demonstrated in the scatterplot (right) ($r = -0.59$; $P < 0.001$).

3.3 Results Part 2: Validation Cohort

3.3.1 Validation Cohort Show Body Composition Features are Largely Independent

Similar to the discovery cohort, the validation cohort demonstrated that the three body composition phenotypes of interest (sarcopenia, myosteatosis and dense sub-q) were observed to be largely independent of one another (56%); however, the proportion of patients with single

body composition features was lower than in the discovery cohort (74%). The overlap of just sarcopenia and myosteatosis was higher at 31% when compared to the discovery cohort's 15%. The concurrence of all three phenotypes was relatively rare (n = 37, 6%), as in the discovery cohort. Myosteatosis and dense subcutaneous were almost mutually exclusive (n = 11, 2%). All overlap can be observed in Figure 3.5.

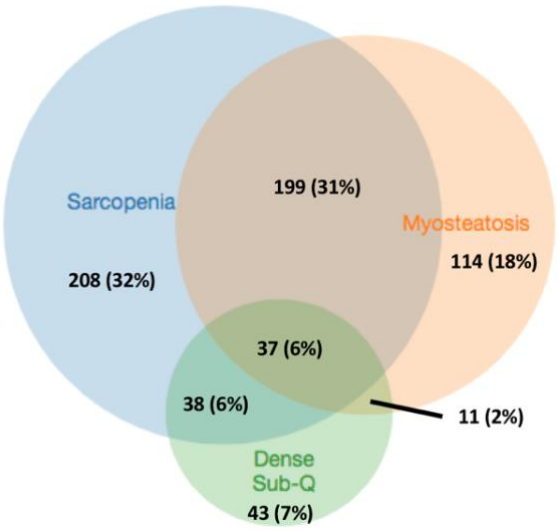

Figure 3.5. Venn diagram displaying phenotypic independence and overlap in validation cohort (N = 650). The three body compositions of interest revealed an independence of 56%.

3.3.2 Clinical Characteristic Differences in the Isolated Phenotypes – Validation Cohort

As the three phenotypes of interest remained largely independent of each other in the validation cohort (56%), clinical characteristics of the independent phenotypes compared to patients with no "abnormal" features were compared. Isolated sarcopenia and myosteatosis groups were both significantly older than patients with no abnormal body composition features ($P < 0.001$ for both). In terms of sex, the no features cohort had a higher proportion of men

(69.7%) than women (30.3%), where isolated sarcopenia and myosteatosis both exhibited a higher representation of females (50.0% and 45.6%, respectively) (P < 0.001, P = 0.003). Conversely, dense sub-q had an even higher representation of males (90.7%) compared to the no features 69.7% male proportion (P < 0.001). All comparisons can be observed in Table 3.3 below.

Variable		No features N = 310	Isolated sarcopenia N = 208	P-value	Isolated myosteatosis N = 114	P-value	Isolated dense sub-q N = 43	P-value
Age	Years	61.0 ± 11.2	65.0 ± 11.8	< 0.001	67.3 ± 11.2	< 0.001	61.3 ± 15.0	0.848
Sex	Females Males	94 (30.3%) 216 (69.7%)	104 (50%) 104 (50%)	< 0.001	52 (45.6) 62 (62.0)	0.003	4 (9.3) 39 (90.7)	0.004
T stage	Stage 1 Stage 2 Stage 3 Stage 4	14 (4.5) 38 (12.3) 216 (67.9) 42 (13.5)	7 (3.4) 28 (13.5) 137 (65.9) 36 (17.3)	0.576	7 (6.1) 11 (9.6) 83 (72.8) 13 (11.4)	0.718	1 (2.3) 7 (16.3) 20 (46.3) 15 (26.3)	0.002
N stage	Stage 0 Stage 1 Stage 2	148 (47.7) 106 (34.2) 56 (18.1)	97 (46.6) 79 (38.0) 32 (15.4)	0.589	57 (50.0) 39 (34.2) 18 (15.8)	0.846	22 (51.2) 14 (32.6) 7 (16.3)	0.910
M stage	No metastasis Metastatic	0 (0) 0 (0)	0 (0) 0 (0)	NA	0 (0) 0 (0)	NA	0 (0) 0 (0)	NA

Table 3.3. Isolated phenotypes (isolated sarcopenia, isolated myosteatosis and isolated dense sub-q) compared to patients exhibiting no "abnormal" body composition phenotypes – validation cohort.

3.3.3 All Three Phenotypes are Influential on Overall Survival Outcomes

The three body composition definitions utilized in the discovery cohort all yielded significant influences on overall survival outcomes upon univariate assessment in the validation cohort (N = 960). Specifically, the log-rank p-values for sarcopenia, myosteatosis and dense sub-q on overall survival outcomes were P = 0.042, P < 0.001 & P < 0.001, respectively. This was particularly important for the cut-point determined for dense subcutaneous adipose tissue (-

87HU) as it was externally validated and is appropriate for generalization to other cohorts. All survival curves can be viewed in Figure 3.6.

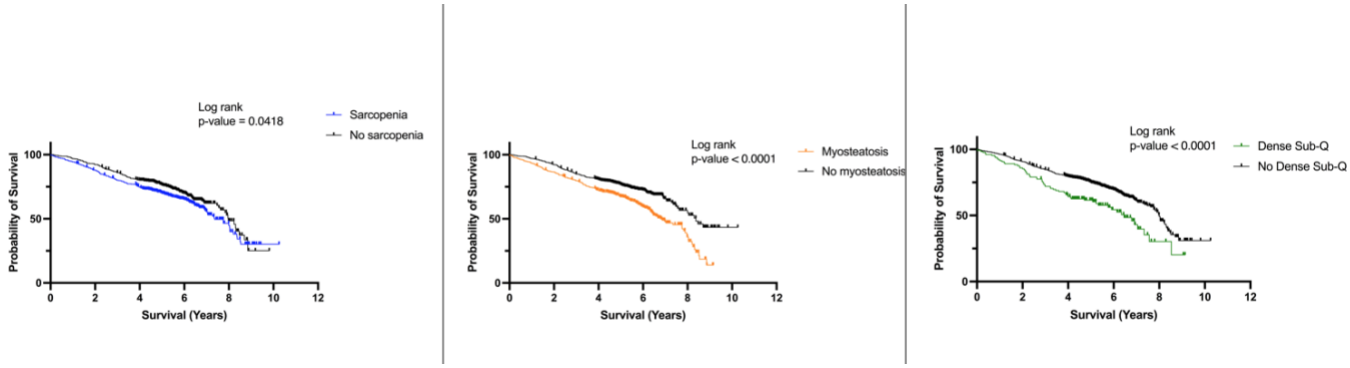

Figure 3.6. Survival curves of sarcopenia (Martin definition), myosteatosis (30 HU) and dense sub-q (-87) in the validation cohort. All three definitions were statistically significant on reducing overall survival as revealed by Kaplan-Meier analyses (P = 0.042 for sarcopenia; P < 0.001 for both myosteatosis and dense sub-q.

3.3.4 Phenotype Overlap Influences Survival Outcomes

The summative influence of the body composition phenotypes was also observed in the validation set, as the presence of at least two or three features yielded the most significant differences in overall survival outcomes compared to one or zero features ($p < 0.001$) (Figure 3.7)

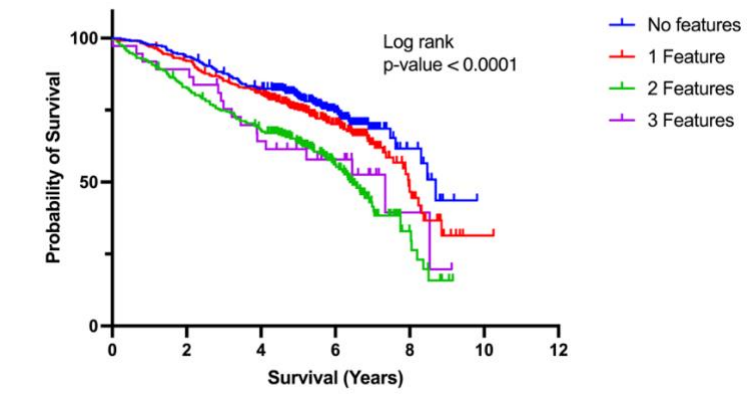

Figure 3.7. Summative influence of overlapping phenotypes on OS – validation cohort. The overlap of two features worsened OS compared to one feature, and three was subsequently worse than two, as revealed by Kaplan-Meier statistical analyses (P < 0.001).

3.3.5 Correlation of SAT Surface Area and Radiodensity

Similar to the discovery cohort, several significant correlations were observed in the validation cohort. SAT surface area and radiodensity demonstrated a negative, curvilinear relationship (r = -0.70, P < 0.001). Lower surface areas were associated with higher adipose tissue radiodensities and similar to the discovery cohort, at approximately 150cm^2, there is a sharp increase in radiodensity (Figure 3.8).

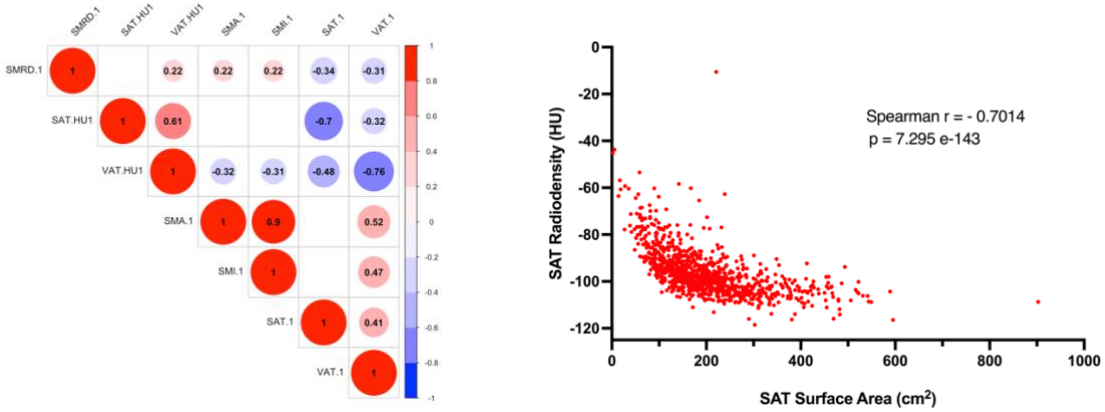

Figure 3.8. Correlation matrix continuous body composition measurements – validation cohort. Spearman rho correlations of continuous body composition values revealed a strong, negative correlation of SAT surface area (cm^2) and SAT radiodensity, demonstrated in the scatterplot (right) (r = -0.70; P < 0.001).

3.3.6 Body Composition Phenotypes are Dependent Upon BMI Status

The validation cohort provided additional information on the influence of BMI status on the body composition phenotypes under assessment. BMI was particularly influential on the myosteatosis and dense subcutaneous phenotypes. Specifically, myosteatosis prevalence and independence increased as the BMI status was increased. An opposite relationship was observed with the dense sub-q phenotype, as its prevalence decreased with higher BMI and at lower BMI's it was highly overlapped with sarcopenia. Sarcopenia remained relatively consistent across BMI categories, but decreased in prevalence at BMIs greater that 30. An overview of the trends can be observed in Figure 3.9 below.

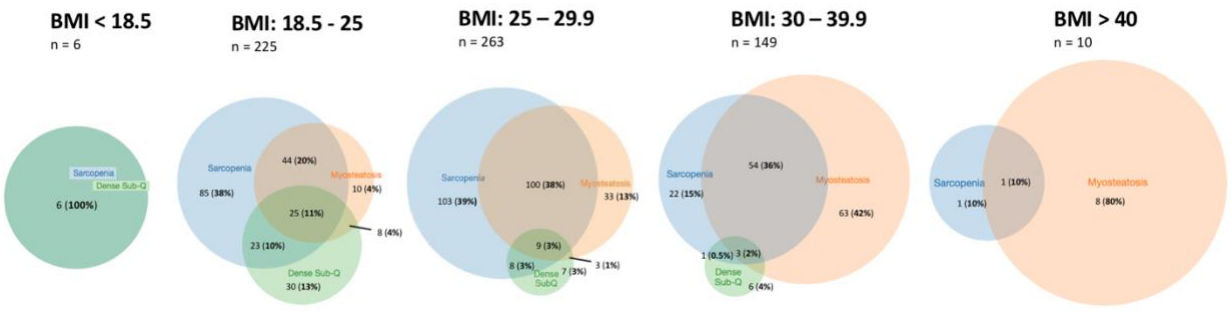

Figure 3.9. Influence of BMI status on sarcopenia, myosteatosis and dense sub-q prevalence, overlap and independence. Myosteatosis increased in prevalence and independence when

transitioning from lower to higher BMI categories, whereas the opposite trend was observed for dense sub-q.

3.4 Discussion

The overarching hypothesis for this aim was that the presence of a colorectal tumor can give rise to three abnormal body composition phenotypes: sarcopenia, myosteatosis and dense sub-q. In addition, it was hypothesized that these features would be independent of each other and be influential on overall survival outcomes. This hypothesis was tested in both a discovery and validation set of patients with CRC. Overall, we confirmed our hypothesis, and main findings are discussed below.

In our discovery and validation cohorts, we examined the overlap of the three BC features under assessment and found that each feature remained relatively independent of one other (74% and 56% independence, respectively). Although overlap exists between the phenotypes, particularly in the validation cohort, the body composition more frequently appear independently. A large bulk of the research conducted on CT-derived body composition phenotypes evaluates them as separate entities (73, 113, 114). To our knowledge, there is no previous work that evaluates the overlap of sarcopenia, myosteatosis and dense sub-q. However, Martin et al. examined the overlap of sarcopenia, myosteatosis and visceral obesity (VO) in a pooled Canadian and UK cohort (N = 2100) (75). This work found a 36% independence between the three features and a 20% overlap between sarcopenia and myosteatosis (similar to the 19% overlap between these two features in our discovery cohort). However, the viscerally obese phenotype limits the applicability of this study to ours as VO is likely a different phenotype from that of dense sub-q; higher adipose tissue surface area is associated with lower fat radiodensities

in the visceral and subcutaneous regions ($r = -0.70$, $P < 0.001$). Certainly, our work addresses a large knowledge gap by investigating the interplay of myosteatosis, sarcopenia and dense subcutaneous adipose tissue, which is increasingly being recognized as a wasting phenotype in cancer (86).

This study also found that myosteatosis and dense sub-q are independent predictors of overall survival ($P < 0.001$, $P = 0.050$) and that sarcopenia was influential on decreasing OS in our validation cohort (and the discovery cohort when phenotypic overlap was removed). This is consistent with other studies which have reported sarcopenia and myosteatosis significantly reduces OS survival outcomes in CRC (34, 73, 74). In addition, dense subcutaneous adipose tissue radiodensity has recently received more attention as having prognostic value. For instance, highly dense subcutaneous adipose tissue has been demonstrated to reduce OS in a population of chemo-refractory advanced CRC (34). In addition, higher subcutaneous fat radiodensities were associated with higher risks of death in a population of stage I – III CRC (N = 3262) (33). These studies, along with our work, demonstrate that there are other influential body composition phenotypes that may develop with or independently of sarcopenia and myosteatosis. Our work also found that there was a summative influence of overlapping phenotypes on OS outcomes. Particularly, with the presence of all three exhibiting particularly poor OS ($p < 0.001$). Other work has shown that the presence of multiple overlapping phenotypes (sarcopenia, myosteatosis and VO) significantly increases length of hospital stay and short-term mortality rates in CRC (75). Perhaps overlapping phenotypes may represent a more severe state of wasting and future work is needed to further delineate the mechanisms of wasting in these conditions.

The influence of BMI on each body composition of interest was explored (Figure 3.9). We observed that sarcopenia remained relatively consistent throughout each BMI category, with highest prevalence occurring at BMI's between 25 – 29.9. Myosteatosis prevalence increased with higher BMI status and independence also increased. This is consistent with other work where myosteatosis was observed at higher BMI's (84). Xiao et al. have also shown that low skeletal muscle radiodensities more frequently occur in patients with higher total adipose tissue surface areas in a population of 3262 patients with CRC (stage I – III) (115). Finally, dense subcutaneous adiposity decreased in prevalence with higher BMI categories and remained independent of myosteatosis (only 2% of individuals only exhibited dense sub-q and myosteatosis) (Figure 3.1 & 3.5). We also show that adipose tissue radiodensity and surface area have a negative relationship, with less surface area leading to higher fat radiodensities (Figures 3.4 & 3.8). The pathophysiology associated with the development of dense subcutaneous adipose tissue is not well understood. It is speculated that increased fat density could be related to a decrease in lipid content in adipocytes, which may be associated with the lipid browning that occurs in cachectic wasting (115, 116). Future work is needed to understand the development of dense sub-q and how it relates to other wasting mechanisms that manifest as sarcopenia and myosteatosis.

This study has a high degree of power and generalizability as we were able to reproduce the findings of the discovery cohort (n = 319) on an external cohort of CRC patients (N = 960). A limitation of this work that should be mentioned is that we didn't examine visceral obesity and the influence it has on the findings we report (other than within our BMI assessments). VO has been shown to decrease survival outcomes and other factors such as length of hospital stay.

However, the measurement of VO can be problematic as the patient's position, in addition to any movement that occurs during the CT imaging process, can often lead to inaccurate quantification of visceral fat surface area (117). In addition, visceral adiposity can be overestimated, as a lot of the tissue within the abdomen (i.e. organs, connective tissue) are the same radiodensity as fat mass (118). Therefore, we only included adipose tissue in the subcutaneous region for interpretation as it is a easily identified, defined area within the CT image.

Another limitation to note is that we had little clinical information regarding other co-morbidities. Without this information, potential confounders that could have also influenced survival outcomes could not be assessed. In addition, limited information was available on neo-adjuvant therapies that may have been given before the surgical resection, which may also have had an impact on body composition based on previous work (19, 21, 22). Future goals for this work will aim to examine the influence of neoadjuvant cancer therapies in relation to body compositions by obtaining more relevant clinical information surrounding this cohort.

Overall, this aim found that three wasting phenotypes are identifiable in CRC: sarcopenia, myosteatosis and dense sub-q. Each is influential on OS outcomes and demonstrate a large degree of independence. BMI is as important factor to consider when assessing these BC phenotypes as myosteatosis occurs more frequently overweight and obese individuals and dense sub-q is more prevalent in normal-to-underweight individuals. Sarcopenia is observable in all BMI categories. Finally, fat radiodensity increases with lower fat surface area and is an important factor to assess when evaluating wasting in patients with cancer.

Chapter 4: Targeted Serum Proteomics

4.1 Introduction

As was demonstrated in the previous chapter, there are three independent body composition phenotypes that are detectable in colorectal cancer. These three body composition features are each influential on overall survival outcomes, which was exemplified in both a discovery and validation cohort. Although these phenotypes are largely distinct from each other (approximately 65% independence on average), the co-existence of multiple phenotypes further adversely affects survival outcomes. There is currently no literature that examines differences in protein concentrations that are related to tumor-mediated wasting in the independent phenotypes of sarcopenia, myosteatosis and dense sub-q. To explore the mechanisms and pathways that may be involved in the pathogenesis of cancer-associated muscle loss, myosteatosis and dense sub-q, 20 circulating features detectable in sera were evaluated in relation to each phenotype.

The known mechanisms of muscle and fat loss in the cancer setting are complex and involve many different pathways. Therefore, to explore whether tumor-mediated wasting mechanisms are involved in relation to the three body composition phenotypes detected in Aim 1 we explored 20 proteins in the pre-operative sera of a subset of the discovery cohort. These 20 proteins were selected based on three overarching physiological functions: inflammation, energy homeostasis and muscle maintenance.

Circulating proteins selected that were involved in inflammatory processes were TNF-α, CRP, cortisol, adipsin, macrophage migration inhibitory factor (MIF), plasminogen activator

inhibitor-1 (PAI-1), lipocalin-2 and heat shock proteins 70/90. These proteins have a wide range of inflammatory functions such as, but not limited to: promoting macrophage function, enhanced proteolysis/lipolysis, inhibition of myoblast differentiation and the promotion of the acute phase response (93-97, 99, 102, 119-122). Proteins related to energy homeostasis were also selected for analysis. These proteins were: ghrelin, leptin, insulin, IGF-1, IGF-2, adiponectin, resistin (98, 103-106). These proteins were selected as they are influential in appetite regulation, management of energy homeostasis, protein synthesis and insulin sensitivity. Muscle maintenance proteins myostatin, follistatin and testosterone were also selected for analysis (107-109). For more detailed description of physiological functions, please refer to Table 2.1 in Chapter 2: Methods.

There is limited work on circulating mediators in tumor-mediated wasting literature in relation to body composition features that have been quantified through human CT scans in CRC. Therefore, this work examined biological correlates of circulating proteins in established wasting models patients with CRC which were quantified by multiplex protein bead assays. We hypothesized that each body composition feature (sarcopenia, myosteatosis and dense sub-q, respectively) would present unique biological correlates with the metabolic and inflammatory mediators that were detected in human sera samples.

In addition to the targeted proteomic analysis described above, shotgun proteomics utilizing tandem mass tag (TMT) labelling was also completed. Unfortunately, this experiment yielded no significant findings. A full methodological description of this experiment and non-significant findings can be reviewed in Appendix A.

4.2 Results

4.2.1 Independent Phenotypes Exhibited Differences in Protein Abundance

Protein concentrations between patients with sarcopenia, myosteatosis, dense sub-q and no features (with no overlap) were first compared. In total, 119 patients had one of these features (by itself): 28 had sarcopenia alone, 28 had myosteatosis alone, 7 had dense sub-q alone, and 56 had none of these features. Not all protein concentrations for the 20 analytes were available for all 119 patients; therefore, the number of patients included for each protein comparison can be observed in Table 3.1. Kruskal-Wallis H test revealed that there were significant differences in three proteins between the four groups, which were leptin ($p < 0.001$), adipsin ($p = 0.002$) and resistin (0.005). After pairwise comparisons, leptin was found to be significantly higher in the myosteatosis phenotype compared to normal, sarcopenia and dense sub-q phenotypes (all p-values < 0.05) and adipsin was higher in the myosteatosis phenotype compared to sarcopenia and no phenotypes (both p-values < 0.05). Resistin was significantly higher in the myosteatosis phenotype compared to the no features group ($p < 0.05$). TNF-α was also shown to be higher in the myosteatosis phenotype; however this did not quite reach statistical significance (p-0.054; Table 4.1).

Protein	Analyte units	Total N	Kruskal-Wallis H-Test Adj. p-value	Kruskal-Wallis H-Test not adj. p-value	None (median value)	Sarcopenia (median value)	P-value (None vs. Sarco)	Myosteatosis (median value)	P-value (None vs. Myo)	Dense Sub-Q Fat (median value)	P-value (Dense vs. None)
CRP	mg/mL	116	0.999	0.215	2.31	1.63	--	2.40	--	1.30	--
TNFα	pg/mL	106	0.999	0.054	4.02	5.37	--	5.24	--	3.24	--
MIF	pg/mL	106	0.999	0.928	385.0	402.4	--	354.1	--	434.5	--
PAI-1	pg/mL	106	0.999	0.139	26960.0	30430.0	--	34794.3	--	30805.8	--
Lipocalin-2	pg/mL	106	0.999	0.256	309949.5	358856.2	--	443797.8	--	469242.8	--
Resistin	pg/mL	106	0.125	0.005	28493.9	36837.8	--	50940.6	0.007	55421.8	--
HSP 90	ng/mL	106	0.999	0.771	13.2	13.5	--	12.7	--	14.7	--
HSP 70	pg/mL	106	0.999	0.426	105846.0	97349.4	--	110316.1	--	88818.8	--
Cortisol	nmol/L	109	0.999	0.329	322.0	358.0	--	305.0	--	411.0	--
Vitamin D	nmol/L	110	0.999	0.292	63.5	61.7	--	56.6	--	72.3	--
Ghrelin	pg/mL	106	0.999	0.554	4.20	4.20	--	5.73	--	6.47	--
Leptin	pg/mL	106	0.001	0.000058	4151.5	4078.1	--	9350.4	0.003	2005.2	--
Insulin	pg/mL	106	0.999	0.168	480.3	539.2	--	626.5	--	373.8	--
IGF-1	pg/mL	106	0.999	0.237	33775.5	34932.2	--	27665.8	--	35343.8	--
IGF-2	pg/mL	106	0.999	0.386	204683.4	153039.1	--	141575.7	--	212815.4	--
Adiponectin	pg/mL	106	0.999	0.999	18660000.0	22412000.0	--	21747000.0	--	25862000.0	--
Adipsin	pg/mL	105	0.028	0.0014	4532700.0	4634700.0	--	7202500.0	0.001	3973100.0	--
Myostatin	pg/mL	106	0.999	0.407	47.6	31.4	--	51.8	--	28.5	--
Follistatin	ng/mL	106	0.999	0.173	0.630	0.610	--	0.610	--	0.845	--
Testosterone	nmol/L	109	0.999	0.094	10.1	10.0	--	1.25	--	14.9	--

Table 4.1. Targeted proteomic analysis in patients with each body composition feature.

4.2.2 Myosteatosis Patients Have a Unique Proteomic Signature

Next, protein concentrations of the 20 analytes were compared between myosteatosis vs all other patients without myosteatosis. Three proteins were significantly different in abundance between the myosteatosis vs no myosteatosis phenotypes after correction for multiple comparisons. Similar to what was observed with the non-parametric ANOVA, the concentration of leptin was significantly higher ($1.12 \times 10^4 \pm 1.07 \times 10^4$ ng/mL) in the myosteatosis phenotype compared to those without myosteatosis ($5.84 \times 10^3 \pm 6.06 \times 10^3$ ng/mL) ($p = 0.0348$). Similarly, adipsin concentrations were significantly higher in the myosteatosis group ($8.33 \times 10^6 \pm 5.24 \times 10^6$ ng/mL) compared to the no myosteatosis cohort ($5.4 \times 10^6 \pm 3.96 \times 10^6$ ng/mL) with $p < 0.05$. Conversely, IGF-1 was found to be lower in concentrations ($3.68 \times 10^4 \pm 1.48 \times 10^4$ ng/mL) in the myosteatosis group compared to those without myosteatosis ($2.76 \times 10^4 \pm 1.40 \times 10^4$ ng/mL), $p = 0.0368$. These differences can be observed in Figure 4.1.

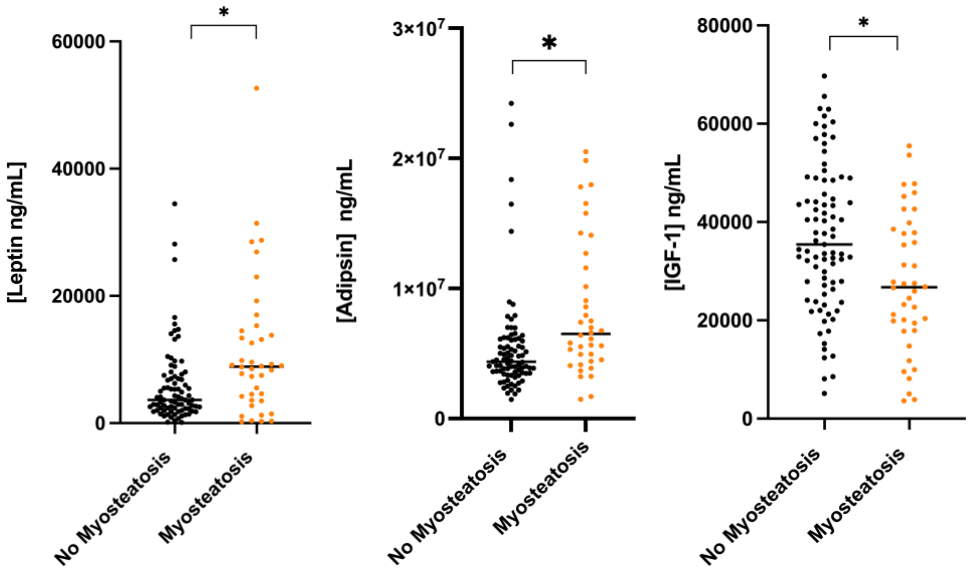

Figure 4.1. Significant protein differences between myosteatosis and no myosteatosis patients. Through Mann-Whitney U tests myosteatosis was revealed to have statistically significantly higher leptin and adipsin as well as reduced IGF-1. P < 0.05 is represented by *.

4.2.3 Proteomic Changes Associated with Dense Sub-Q

The same tests were performed on patients with dense sub-q compared to those without dense sub-q. Only one protein was statistically significant, which was leptin. Leptin was significantly decreased ($2.71 \times 10^3 \pm 2.72 \times 10^3$ ng/mL) in patients with dense sub-q compared to those without ($8.16 \times 10^3 \pm 8.47 \times 10^3$ ng/mL) p = 0.0326 (Figure 4.2). No differences in protein concentration were observed in patients with sarcopenia compared to patients without sarcopenia.

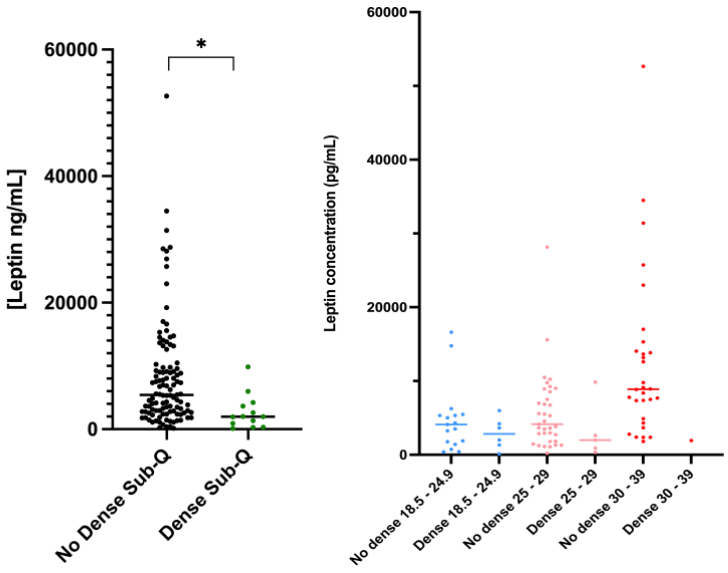

Figure 4.2. Leptin concentrations in patients with dense sub-q, in addition to BMI influence. Dense Sub-Q has significantly reduced concentrations of circulating leptin, as revealed by Mann-Whitney U testing. P < 0.05 is represented by *.

4.2.4 BMI Status Influences Protein Concentrations in Myosteatosis and Dense Sub-Q

In Aim 1 it was revealed that myosteatosis and dense sub-q are influenced by BMI status. Therefore, the influence of BMI status was then explored for the significantly different proteins in the myosteatosis and dense sub-q phenotypes. Specifically, leptin concentrations remained similar between the myosteatosis and no myosteatosis phenotypes in BMI's between 18.5 and 29; however, leptin concentration was significantly higher in the myosteatosis phenotype compared to no myosteatosis in obese individuals with BMI's between 30 – 39, p = 0.03. Adipsin concentrations remained higher in patients with myosteatosis consistently across all BMI categories. IGF-1 remained consistently lower in myosteatosis groups across all BMI categories; however, this trend was not statically significant after multiple comparisons. Finally, leptin was

consistently lower in patients with dense subcutaneous adipose tissue, although significance was not observed (Figures 4.2 & 4.3).

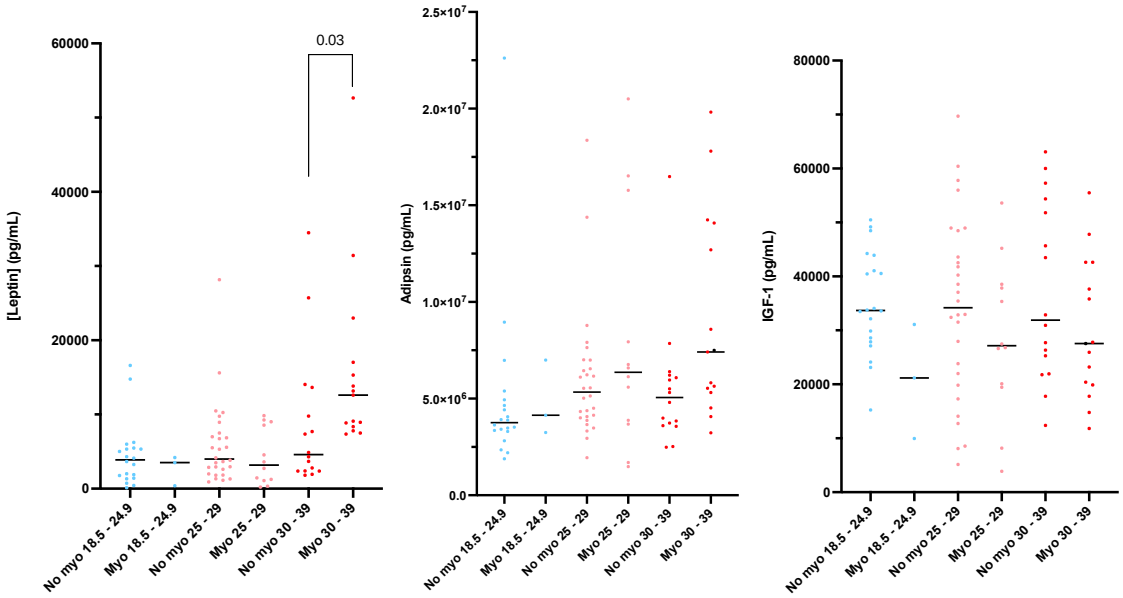

Figure 4.3 Influence of BMI status on concentrations of leptin, IGF-1 and adipsin in patients with and without myosteatosis. Mann-Whitney U testing revealed patients with myosteatosis whom also had a BMI greater than 30 had significantly higher concentrations of circulating leptin (P = 0.030).

4.2.5 Biological Correlates Between Continuous Body Composition Measures and Protein Concentrations

Spearman rho correlations were completed separately for males and females between continuous body composition measurements and protein concentrations. After adjustment for multiple comparisons, subcutaneous adipose tissue radiodensity was negatively correlated with leptin concentrations in both males ($r = -0.449$, $p < 0.05$) and females ($r = -0.636$, $p < 0.01$). In females only, skeletal muscle radiodensity was positively correlated with IGF-2 ($r = 0.468$, $p <$

0.01) and was negatively correlated with adipsin (r = -0.456, p = 0.02). Correlation plots for both males and females can be observed in Figure 3.4.

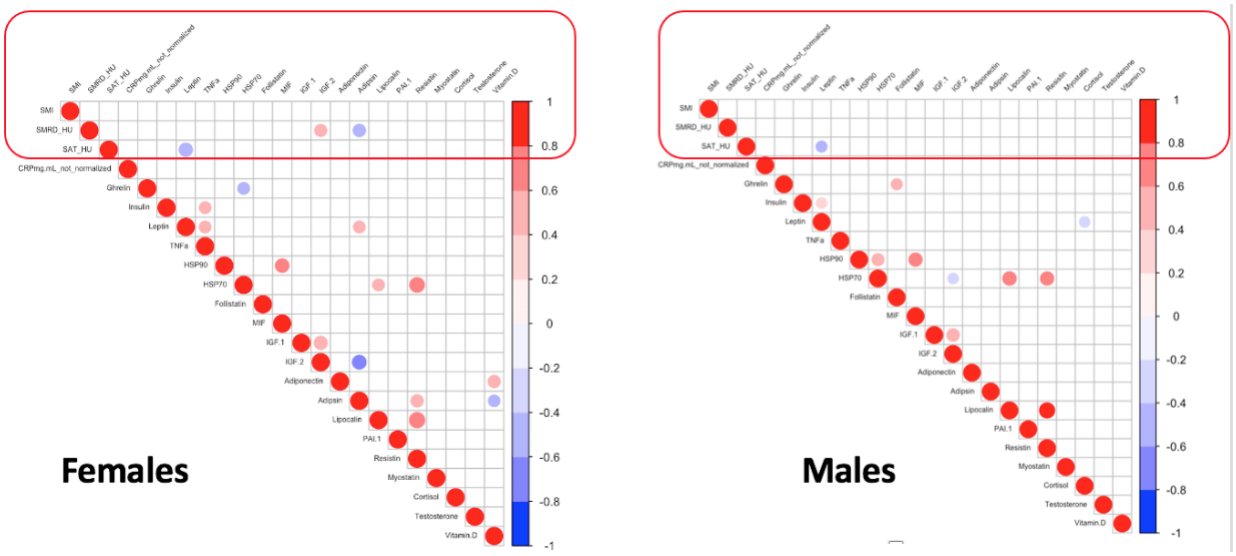

Figure 4.4. Correlation matrices of continuous body composition measurements against protein concentrations dichotomized by sex. Spearman rho correlations revealed SAT radiodensity (HU) is negatively correlated with leptin in males and females and skeletal muscle radiodensity is positively correlated with IGF2 and negatively correlated with adipsin in females. Strength and p-values associated with each correlation represented by the colour and size of the circle. All correlations are corrected for multiple comparisons.

4.2.6 Multivariate Assessment of Proteins in Independent Body Composition Phenotypes

Finally, through multivariate PLS-DA analysis it was determined that the four independent phenotypes (sarcopenia, myosteatosis, dense sub-q and no features) could not be distinguished from each other by the 20 proteins, or through a VIP > 1 filtration. However, slight separation could be observed between the myosteatosis vs. no feature phenotypes,

which gave a weak model consisting of 8 proteins after a VIP > 1 filtration with a R^2Y score = 0.302, Q^2Y score = 0.169 and a CV-ANOVA = 0.02. (Figure 4.5)

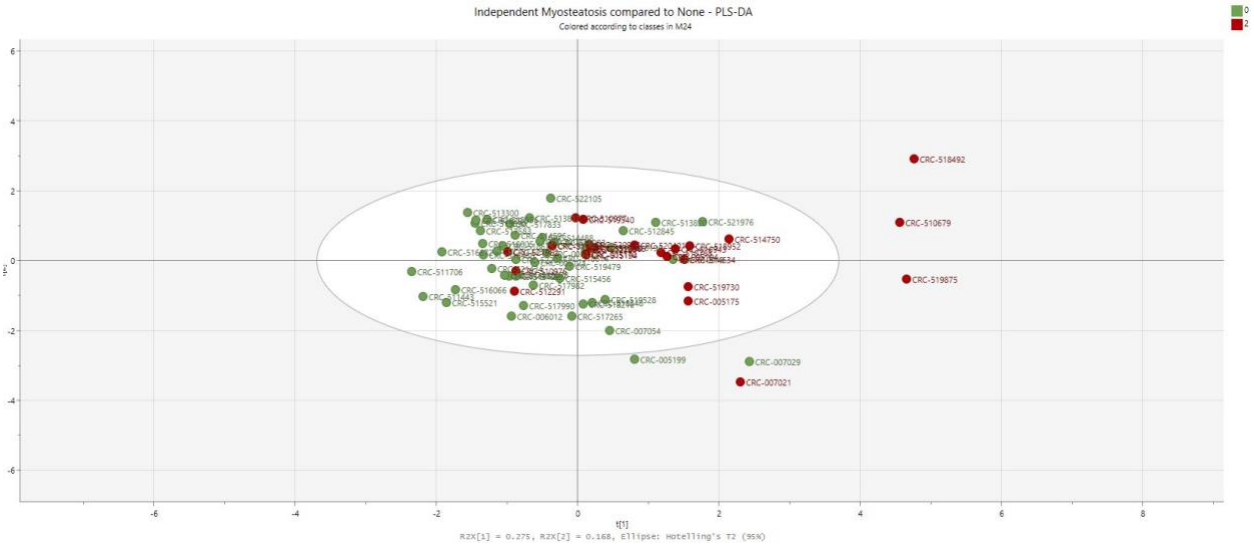

Figure 4.5. PLS-DA of independent myosteatosis (red) and no features (green). Model consists of 8 proteins that gives an R^2Y score = 0.302 and Q^2Y score = 0.169 (P = 0.020).

Within this model, myosteatosis was positively associated with leptin, TNF-α, HSP70, adipsin, PAI-1 and resistin and negatively associated with IGF-2 and testosterone. This can all be observed in the loadings plot below.

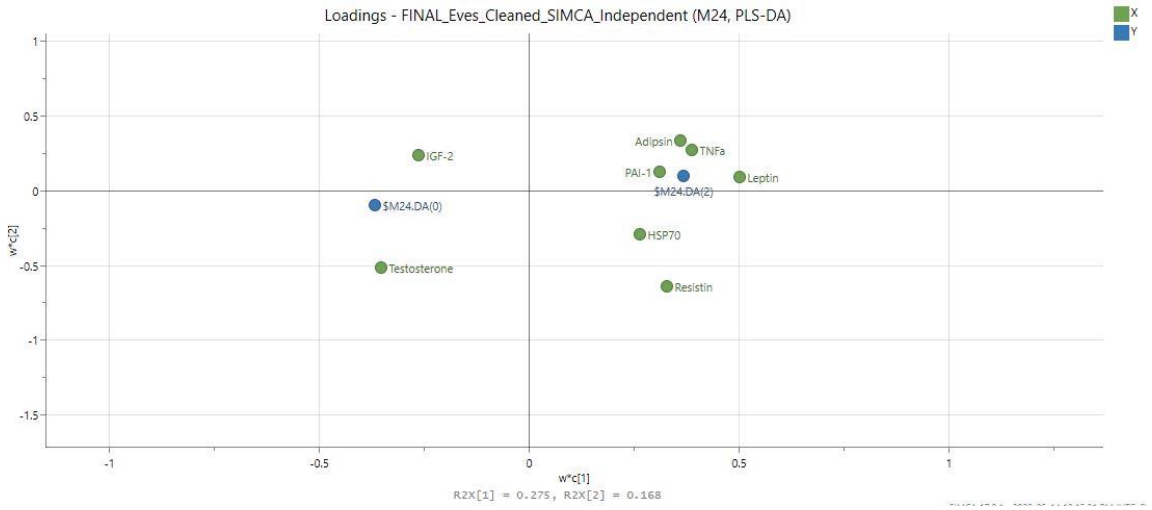

Figure 4.6. Loadings plot of independent myosteatosis vs. no features associated with the PLS-DA above (Figure 4.5). 8 proteins were used to generate this model, and proteins that are highly influential in describing the phenotype of interest are found in closer proximity to phenotype (Y in blue).

4.3 Discussion

The concentration of several circulating features that have been established in cancer cachexia wasting models were explored in three body composition features in colorectal cancer. Circulating proteomic factors in sera were quantified through Multiplexing LASER Bead Technologies and between-phenotype comparisons of cytokine concentrations were conducted via Kruskal-Wallis, Mann-Whitney U and spearman rho statistics. Multivariate analyses were also conducted using partial least squares discriminant analysis. Overall, we found several perturbed proteins in the myosteatosis phenotype and decreased leptin and increased resistin concentrations in the dense sub-q phenotype.

Ectopic lipid accumulation in muscle, or myosteatosis, has been observed in disorders such as obesity or insulin resistance where there is an upregulation of lipolysis within adipose tissue (84). Lipids are then released into circulation; however, at high concentrations of circulating lipids lipotoxicity can occur. Lipotoxicity in the muscle setting occurs when there is a high abundance of FFAs in the tissue that skeletal muscle cannot keep up with the metabolic demands and excess FFAs get stored as lipid droplets (123). We observed elevated levels of three

proteins that promote elevated lipolysis in our cohort of patients with myosteatosis: increased leptin, resistin and TNF-α.

In terms of energy homeostasis mediators, the myosteatosis cohort was shown to have elevated leptin, which was particularly high in obese patients with (BMIs between 30 – 39) ($p = 0.03$). Leptin is positively correlated with adipose tissue surface area; therefore, obese individuals typically have higher abundances of circulating leptin (124). However, because obese myosteatosis patients had even higher levels of circulating leptin compared to obese patients without myosteatosis suggests that leptin may be playing an abnormal role in this phenotype (Figure 4.3). Leptin is known to be released from adipose tissue stores and cause an increase in lipolysis of triacylglycerides, releasing free fatty acids (FFAs) into circulation (125). In addition to leptin, independent myosteatosis was associated with increased resistin which also stimulates lipolysis in adipose tissue (126). Perhaps the increase in adipokines responsible for enhanced lipolysis may be partially responsible for lipid accumulation in muscle, or lipotoxicity. This may be tumor related as peritumoral adipose tissue has been shown to release several adipokines which promote tumor growth (127).

In addition to leptin's metabolic influence on energy homeostasis, this cytokine also has a proinflammatory effect. More specifically, leptin has been shown to induce the release of several proinflammatory cytokines, such as TNF-α (128). Conversely, exogenous supplementation of TNF-a also stimulates the increase of leptin (51). Interestingly, we did observe elevated TNF-α in our independent myosteatosis phenotype (Table 4.1), and TNF-α was positively associated with myosteatosis in the PLS-DA model. Elevated TNF-α, along with other

tumor-mediated proinflammatory responses, elicits the onset of chronic systemic inflammation (23). This may help explain the decrease in IGF-1 observed in our myosteatosis phenotype, which was consistently observed across all BMI categories. Decreased circulating IGF-1 has been documented in cancer settings in associated with the onset of inflammatory host environments (57). It also adds an additional explanation as to why elevated resistin was observed in the myosteatosis phenotype, as this protein has been shown to be associated with insulin resistance (129).

In addition to the inflammatory processes perpetuated by tumor-derived cytokines, inflammation from the complement system is emerging as another player in cancer-associated tissue wasting (130). Circulating adipsin was observed to be elevated in patients with myosteatosis ($p < 0.05$). Adipsin, also known as complement factor D, aids in the activation of the alternative pathway of the complement system which increases phagocytosis potential of macrophages as well as promotes the release of proinflammatory cytokines (131). Deng (2021) observed that cachectic patients with pancreatic cancer exhibited higher abundance of complement factors and that the complement system further perpetuates systemic inflammation in cancer (130). Therefore, the elevated adipsin observed in the myosteatosis phenotype may be a reflection of enhanced inflammatory processes.

Patients with dense sub-q exhibited reduced circulating leptin, opposite of what was observed in the myosteatosis phenotype. As was described in Aim 1, the dense sub-q phenotype is associated with reduced subcutaneous adipose tissue surface area and was more frequently observed in lower BMI categories (Figure 4.2). As such, lower adipose tissue surface area is

associated with lower leptin concentrations in circulation, which may be why this phenotype exhibits reduced circulating leptin (124).

It is important to note that this portion of the study is limited by smaller sample sizes in some of the body composition phenotypes, specifically the independent dense sub-q phenotype (N = 7). This is due to two factors. First, the dense sub-q phenotype is already a small and relatively rare phenotype (N = 40) within the entire 319 patient cohort. Second, not all patients had pre-operative serum available for analysis, and the ones that did needed to have their blood draw date and the CT scan within 100 days of each other in order to be included in the study. Some date differences exceeded the 100 day criteria and had to be excluded, leaving our 140 patients that did have sera that met our criteria left for examination (which were further subcategorized based on their body composition statuses).

Overall, this study is the first to identify elevated leptin, adipsin and resistin in CRC patients with myosteatosis. These proteins are involved in inflammatory and metabolic functions, which demonstrates alterations are occurring in patients with the myosteatosis phenotype. The decreased IGF-1 in the myosteatosis phenotype also suggests a decrease in the anabolic response as seen in tumor-mediated skeletal muscle wasting. This work is also the first to identify perturbed proteins in dense sub-q adipose tissue. These results demonstrate that myosteatosis and dense sub-q are related to factors in models of cancer-associated tissue wasting, which helps support the notion that further work is both important and necessary to examine where these phenotypes fit into cachexia models.

Chapter 5: Untargeted Tumor Proteomics

5.1 Introduction

As was exemplified in Aim 1, there are three biologically independent body composition phenotypes that are detrimental to overall survival outcomes in patients with CRC. In Aim 2, targeted serum proteomics was conducted with 20 features that were selected to give a well-rounded profile of factors related to inflammation, energy homeostasis and muscle maintenance. It was demonstrated that biological correlates existed between the myosteatosis/dense sub-q fat phenotypes and some circulating proteins. Specifically, circulating features related to inflammation and enhanced lipolysis of adipose tissue were particularly prevalent in the myosteatosis phenotype. To supplement these findings, we were interested in conducting untargeted tumor proteomics with the intention of detecting new tumor-associated proteins that may be related to myosteatosis and sarcopenia development.

It has been suggested that mediators originating from the tumor may initiate and sustain muscle and fat wasting (132). Tumors have been shown to secrete a number of factors, some of which are related to wasting. Examples include, heat-shock proteins 70/90, activin A and myostatin, leukemia inhibitory factor, parathyroid hormone (89, 133-136). Although this list is not exhaustive, it helps to exemplify the complexity of cancer-associated atrophy as each of these extracellular factors have differing mechanistic actions ranging from immune system involvement to metabolic derangements. In addition to factors secreted by the tumor, metabolic perturbations within cancer cells that ultimately lead to their enhanced proliferation and survival can lead to downstream wasting effects. For instance, it has been well described that tumors can

release inflammatory mediators and other metabolic players that ultimately lead to the upregulation of mobilized lipid and amino acids in the blood stream that arise from adipose tissue and skeletal muscle (23). Indeed, the presence of a tumor wreaks havoc on the metabolic and inflammatory state of the patient, making this disease incredibly complex. This makes the development of treatment options difficult as there are many physiological pathways involved. Until a fully inclusive, comprehensive model of tumor-mediated wasting is developed, treatment options remain elusive. Therefore, the need to identify additional perturbed physiological pathways and associated tumor-derived proteins is important to supplement existing wasting models that will help guide the development of potential treatment options.

The use of proteomic methods is one such way to explore tumor-derived factors as Omics methodologies are continuing to emerge as important research tools in evaluating biological changes that occur in association with cancer (137). Proteomic analyses allow for the evaluation of full protein sets from samples such as tissue, serum or individual cells which is especially helpful in identifying novel biomarkers that may not been previously considered or explored. Therefore, the purpose of this aim was to perform label-free proteomic experiments utilizing LC-MS/MS on CRC tumors from patients with either sarcopenia and myosteatosis and compare them to control samples of patients with no wasted phenotypes. In addition, we also wanted to determine if the three phenotypes could be separated based on differences in protein abundance based on multivariate partial least squares discriminant analysis. We hypothesized that there would be differences in protein abundance between the three phenotypes, which would be a reflection of physiological pathway perturbations.

5.2 Results

5.2.1 DEP: Sarcopenia vs Normal

After imputation for missing values was performed, differential abundance analysis revealed 7 significantly different proteins between the sarcopenia and normal body compositions. Only one was more abundant in the sarcopenia phenotype, which was Phosphatidylinositol Transfer Protein Beta (PITPNB). The other 6 proteins were more abundant in the normal phenotype, which were Tryptase 2 beta (TPSB2), Latent TGF-B binding protein 4 (LTBP4), Short chain acyl-CoA dehydrogenase (ACADS), Creatine Kinase, Mitochondrial 1A (CKMT1) and histone clusters Hist1h1b and Hist1h2br. These proteins are likely related to metabolic and inflammatory processes in addition to cell transport. The volcano plot and heatmap to these proteins can be viewed in Figure 5.1.

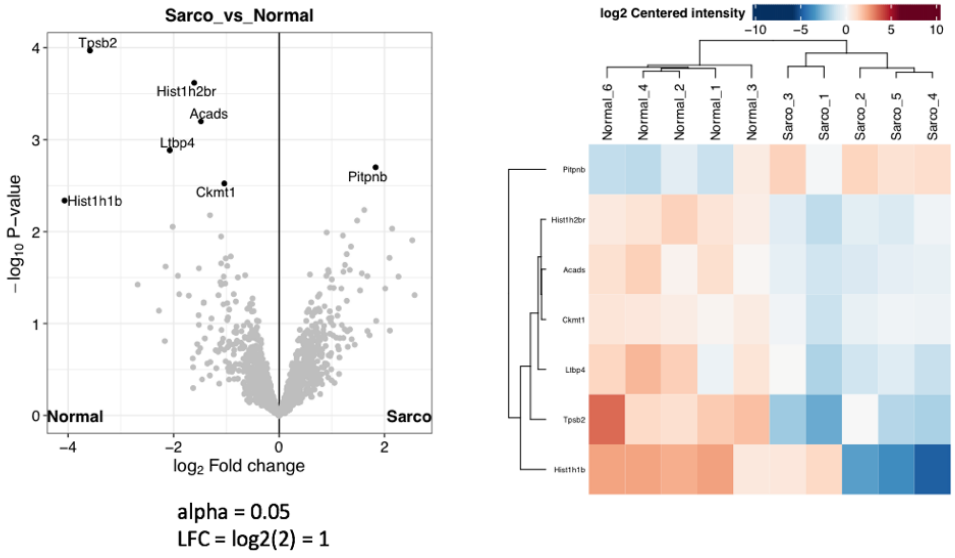

Figure 5.1. Volcano plot and heatmap of differentially abundant proteins in Sarcopenia vs Normal. Seven statistically significant proteins were identified at P < 0.05; specifically, one

was differently abundant in sarcopenia and six were differentially abundant in the normal phenotype.

5.2.2 DEP: Myosteatosis vs. Normal

At the $\log_2(2) = 1$ fold change level ($P < 0.05$), there were three proteins that were differentially abundant between the myosteatosis and normal phenotypes. Specifically, Glyoxalase 1 (Glo1) and Adenylate kinase isoenzyme 1 (Ak1) were higher in abundance in the myosteatosis phenotype and NADH dehydrogenase 1 alpha subcomplex 13 (Ndufa13) was lower (Figure 5.2). All three proteins are associated with metabolic processes.

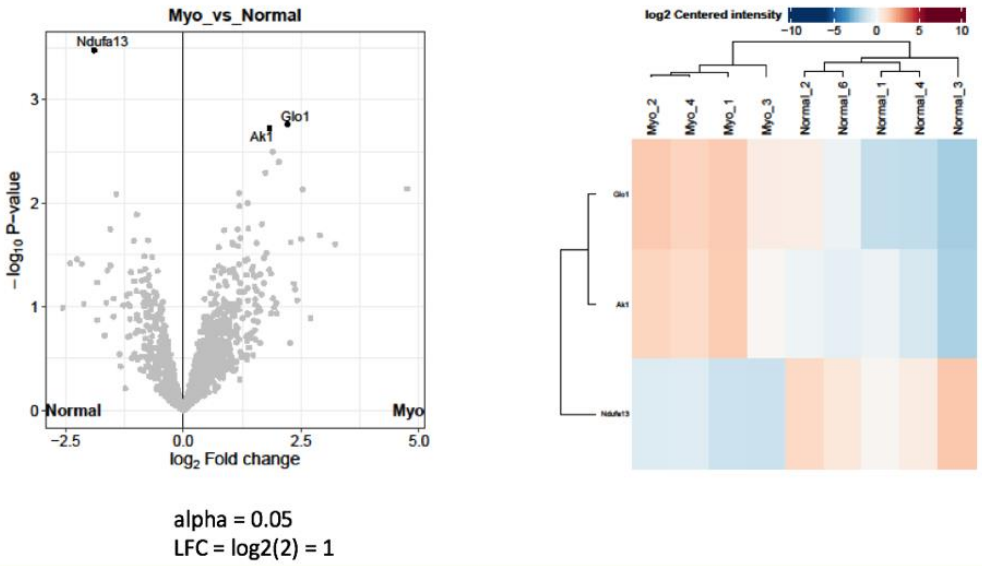

Figure 5.2. Volcano plot and heatmap of differentially abundant proteins in myosteatosis vs normal. Three statistically significant proteins were identified at $P < 0.05$; specifically, two were differentially abundance in the normal phenotype and one in the myosteatosis phenotype.

5.2.3 Partial Least Squares-Discriminant Analysis

PCA (to check for potential outliers) coupled with PLS-DA analysis was utilized to determine if between-group differences could be observed utilizing the proteins detected by the LC-MS/MS. The LC-MS/MS detected 1545 proteins that were imported into SIMCA for analysis. The PCA demonstrated that none of the 14 patient cohort were outliers and all were included in the analysis (Figure 5.5).

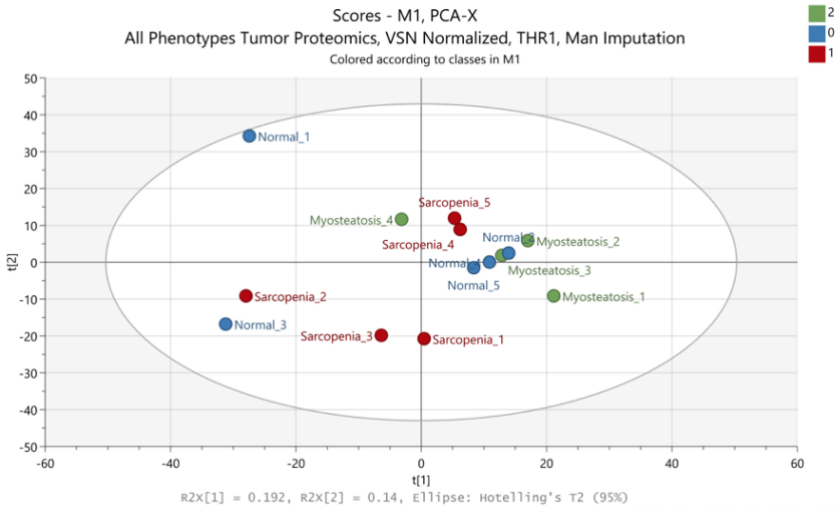

Figure 5.3. PCA of all independent phenotypes (N = 14). PCA diagrams plot individual samples as clusters of samples based on their physiological similarities. As such, a random pattern indicates no inherent bias exist within the data, therefore we proceeded with further statistical analyses including all samples.

After the PCA analysis, the entire cohort was included in the development of a parsimonious PLS-DA model that was created by filtering for VIP's > 1. A total of 33 proteins were included in the final model, which consisted of: R^2Y score = 0.995, Q^2Y score = 0.925 and a CV-ANOVA = 0.02 (Figure 5.4). A loadings plot demonstrated that 11 proteins were positively

associated with the normal phenotype, 10 proteins were positively associated with sarcopenia and 12 with myosteatosis (Figure 5.7).

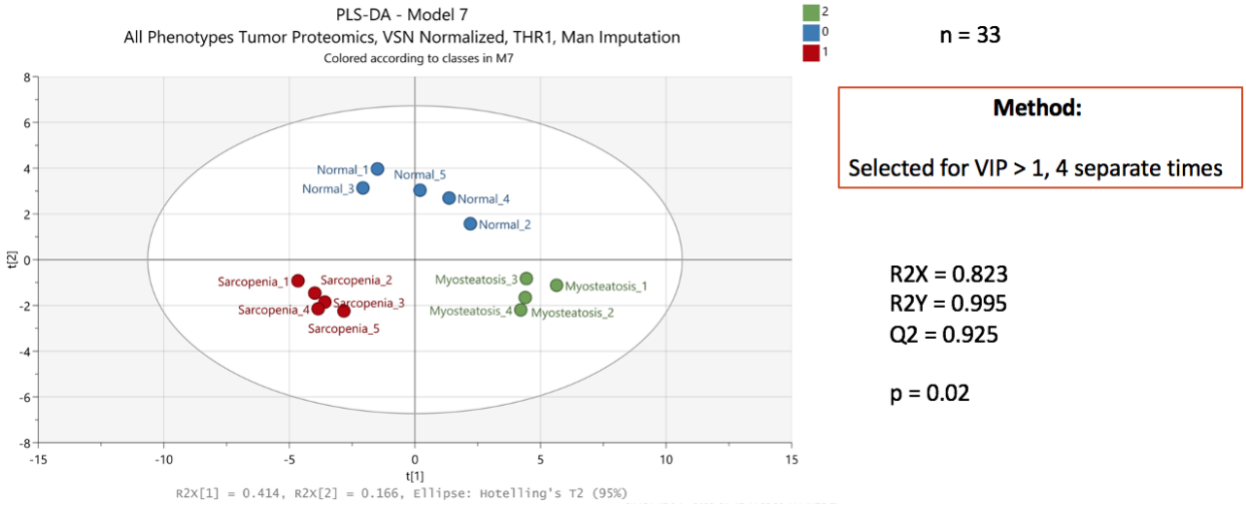

Figure 5.4. PLS-DA of all independent phenotypes of interest. Proteins were filtered via a method of including proteins with a variable influence of projection (VIP) greater than 1. A large degree of separation between phenotypes was observed ($R^2X = 0.823$; $R^2Y = 0.995$; P = 0.02).

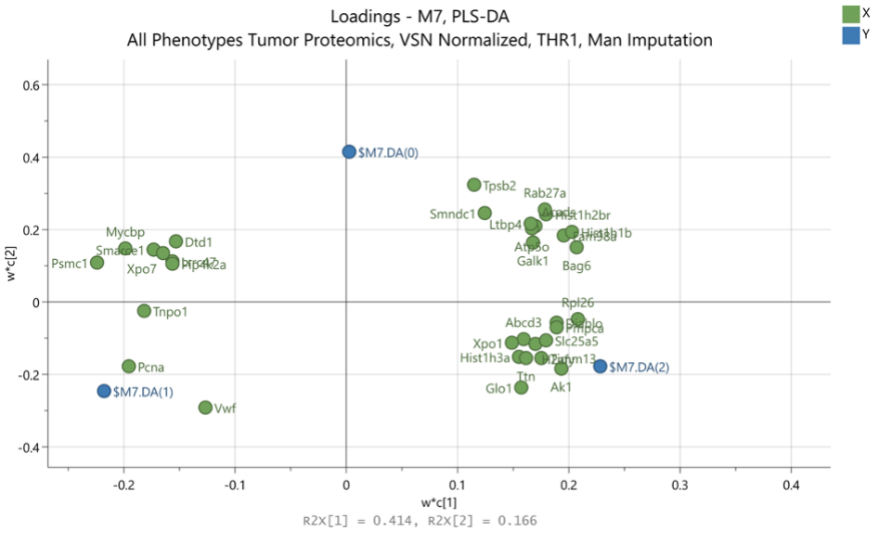

Figure 5.5. Loadings plot associated with the PLS-DA for independent phenotypes above (Figure 5.4). 33 proteins were used to generate this model, and proteins that are highly influential in describing the phenotype of interest are found in closer proximity to phenotype (Y in blue).

Of the 33 proteins detected, a positive or negative association to either sarcopenia or myosteatosis compared to normal is described in the table below, in addition to brief physiological functions (Table 5.1).

Protein ID	Coefficient Direction (from loadings plot)			Function
	Myosteatosis	Sarcopenia	Normal	
ABCD3	Negative		Positive	Transfers fatty acids from cytosol to peroxisome lumen for beta-oxidation (138)
ACADS		Negative	Positive	Catalyzes first step of mitochondrial beta oxidation (139)
AK1	Positive		Negative	Aids adenine nucleotide metabolism and energy homeostasis (140)
ATP5O	Negative	Negative	Positive	Mitochondrial membrane ATP synthase, rotational mechanism (141)
BAG6		Negative	Positive	A central regulator of heat shock protein 70 (142)
DIABLO	Negative		Positive	Involved in the activation of apoptosis (143)
DTD1	Negative		Positive	DNA regulation (144)
FAM98a	Negative	Negative	Positive	Promotes colorectal cancer cell malignancy (145)
GALK1	Negative	Negative	Positive	Catalyses first step of galactose degradation (146)
GLO1	Positive		Negative	Detoxifies a-oxoaldehydes which are biproducts of enhanced glycolysis (147)
H2AFY	Positive		Negative	Histone H2A variant; observed to be positively correlated with immune filtration in cancer (148)
HIST1H1B		Negative	Positive	Histone H1.5; chromatin modelling (149)
HIST1H3A	Positive		Negative	Core nucleosome component (150)
LTBP4		Negative	Positive	Regulates TGF-B and renders it unavailable to bind to TGF-B binding site (151)

MYCBP	Negative	Negative	Positive	Positively correlated with beta-catenin expression, which promotes wnt signalling, can can promote muscle growth (152, 153)
PCNA		Positive	Negative	Aids in DNA replication (154)
PIP4K2A	Negative	Positive	Positive	Supresses insulin signalling (155)
PMPCA	Positive	Negative		Involved in protein targeting to mitochondria (156)
PSMC1	Negative		Positive	Component of the 26S proteasome, involved in ubiquitin protein degradation (157)
RAB27A		Negative	Positive	Enhances PI3K/MAPK signalling (158)
RPL26		Negative	Positive	Component of the large ribosomal subunit (159)
SLC25A5	Positive		Negative	Positive regulator of mitophagy (160)
SMARCE1	Negative	Negative	Positive	SWI/SNF complex-related chromatin remodelling; usually act as tumor suppressors, and loss of function associated with malignant transformation (161)
SMNDC1		Negative	Positive	Spliceosome assembly; a deficiency in survival motor neuron associated with reduced myoblast fusion (162)
TIMM13	Positive		Negative	Mitochondrial transport protein (163)
TNPO1	Negative		Positive	Involved in nuclear localization and activation of ROS-related FOXO activation (164)
TPSB2		Negative	Positive	Major protease present in mast cells and released by the coupled activation-degranulation response (165)
TTN	Positive		Negative	Key component of striated muscle (166)
VWF		Positive	Negative	Important for the maintenance of hemostasis (167)
XPO1		Positive	Negative	Has been linked to the enhancement of cytokines related to E3 ubiquitin ligase Atrogin-1 (168)
XPO7	Negative		Positive	Small nuclear transport protein (169)

Table 5.1. Protein descriptions from PLS-DA model and directionality associated with each phenotype.

5.3 Discussion

The purpose of this aim was to identify proteins through label-free quantification via LS-MS/MS that were specific to the independent phenotypes of sarcopenia and myosteatosis when compared to patients with no abnormal BC features. In addition, we were interested in evaluating whether the three independent phenotypes could be separated through differences in protein abundance using a multivariate Partial Least Squares Discriminant Analysis method. We hypothesized that specific proteins would be differentially abundant between the phenotypes and this was confirmed in our findings. Here we describe the potential relevance of some of the interesting protein hits we found based on existing literature.

Utilizing the Bioconductor package "DEP", we identified 7 differentially abundant proteins between the sarcopenia and normal phenotypes. The overall functions of the 7 proteins ranged from participation in inflammatory and metabolic processes to cell transport and histones (Table 5.1). A protein related to inflammation included Latent TGF-B binding protein. We demonstrated that LTBP4 is higher in abundance in the normal phenotype. LTBP4 has been shown to regulate TGF-beta by rendering it unavailable to bind to the TGF-beta binding site (151). This is important as elevated TGF-beta has been documented within wasting models and induces muscle atrophy (170). Although limited work has been completed that evaluates LTBP4 in the cancer setting, overexpression of LTBP4 was found to be associated with greater muscle mass and strength in a mouse model of muscular dystrophy though a mechanism of binding and inactivating myostatin and TGF-beta (171).

Proteins related to metabolic processes were also different in abundance between the sarcopenia and normal phenotypes. For instance, short chain acyl-CoA dehydrogenase was higher in the normal phenotype and is involved the mitochondria metabolism, specifically beta-

oxidation of fatty acids (172). There is no work that has been done to examine the relationship between ACADS and cancer-associated cachectic wasting. However, a recent study demonstrated that decreased expression of ACADS was associated with worsened CRC survival outcomes and that increased expression of ACADS was positively correlated with CD8+ T cells, which are known to produce an anti-tumoral immune response (172). Creatine kinase U from the mitochondria was shown to be lower abundance in patients with sarcopenia. This protein is related to mitochondrial metabolism through the transfer of a phosphate from ATP through phosphocreatine biosynthesis (163). Specifically, a decrease in the creatine-phosphate system (CKS) has been shown to occur in patients with CRC with a subsequent increase in oxidative phosphorylation (173). Perhaps this decrease in the CKS system with relation to the sarcopenia phenotype is related to metabolic changes that enhance muscle wasting in CRC.

The myosteatosis phenotype had higher abundance of glyoxalase I (GLO1) and adenylate kinase isoenzyme 1 (AK1). GLO1 is an enzyme involved in the glyoxalase system, which detoxifies a-oxoaldehydes, such as methylglyoxal, that are produced as side products of enhanced glycolysis (associated with the Warburg effect) (147). Increased production of a-oxoaldehydes contribute to the development of “advanced glycation end products” (AGEs), which have been shown to induce oxidative damage and expression of pro-inflammatory cytokines through receptors for AGEs (RAGE) (147). The elevated abundance of GLO1 in myosteatosis may be a representation of enhanced oxidative stress/inflammation in this phenotype. Elevated AK1 was also observed in the myosteatosis phenotype. AK1 is involved in *de novo* adenine nucleotide synthesis and aids in the maintenance of the balance between AMP, ADP and ATP (174). AK1 manufactures AMP, which is a regulator of the cellular energetics. Elevated AMP produces a regulatory response in

several ways, one of which is via activation of adenosine monophosphate protein kinase (AMPK) signalling which helps to adapt to cellular stress (174). However, elevated AMPK has been shown to induce muscle degradation by inhibiting mTORC1 signalling (175). Therefore, myosteatosis may be influenced by enhanced activation of AMPK signalling.

Finally, a decrease in NDUFA13 was observed in the myosteatosis phenotype. A deficiency in NDUFA13 (a subunit of complex 1 of the electron transport chain) triggers an electron leak from complex 1 (176). This electron leak leads to the development of H_20_2, which leads to peroxiredoxin 2 which can cause STAT3 dimerization (176). As such, elevated STAT3 signalling releases downstream cytokines such as IL-6 and TNF-α (177). Both are pro-inflammatory cytokines that are involved in muscle wasting within the cachexia model. IL-6 and TNF-α both cause an increase in circulating FFA's within patients with cachexia, which may contribute to the ectopic placement of lipids in skeletal muscle tissue (177).

We also demonstrated that these three body composition phenotypes can be separated from each other using multivariate modelling systems such as PLS-DA, where we found 33 proteins that were influential on stratifying the groups. The overall functions of these detected proteins can be viewed in Table 5.1. The proteins had a wide range of physiological functions. An interesting finding related to the sarcopenia phenotype was a positive association with exportin-1. Exportin-1 has been linked to the enhancement of cytokines related to the promotion of E3 ubiquitin ligase Atrogin-1 production, which plays a role in skeletal muscle degradation (168). In terms of myosteatosis, it was shown that ABCD3 was negatively associated with this phenotype. ABCD3 is responsible for the transfer of long-fatty acids from cytosol to peroxisome lumen for

beta-oxidation, which may be a reflection of reduced lipid oxidation previously observed in myosteatosis (32, 138).

Overall, in a univariate approach we found 11 differentially abundant proteins using the Bioconductor DEP package: 7 within the sarcopenia vs. normal comparison and 3 within the myosteatosis vs. normal comparison. These proteins had a range of functions ranging from inflammation to metabolism. We also showed that sarcopenia, myosteatosis and no wasting phenotypes can be separated from each other via multivariate analysis. Further work is needed to elucidate tumor-mediated mechanisms that drive host wasting, as this work was exploratory and is limited by sample size and by having only male subjects. However, this work is helpful in demonstrating the importance of evaluating the proteome in tumor-associated wasting as newly described targets continue to supplement wasting models.

Chapter 6: Discussion / Concluding Remarks

Cancer-associated tissue wasting is a barrier to improving survival outcomes in cancer populations and is also influential on reducing overall quality of life (23). Classical definitions of tissue wasting, or cachexia, are heavily biased towards muscle wasting/low muscle mass (sarcopenia); however, there has been an influx of findings in cachexia research that show additional body composition phenotypes, such as myosteatosis, are also influential on clinical outcomes in cancer populations (30, 40, 72, 73, 75). Such additions to the field helped shape our hypothesis that cachexia, or tumor-associated tissue wasting, may manifest as different body composition phenotypes beyond that of sarcopenia and weight loss. Therefore, the purpose of this work was to evaluate BC status in 319 patients with colorectal adenocarcinoma, as well as conduct proteomic experiments on associated tumor and sera samples, all with the intention of obtaining a better understanding of tumor-mediated muscle and adipose tissue wasting. Findings of the CT portion of this work were then validated on an external dataset of 960 patients with CRC. Overall, we identified three body composition features (sarcopenia, myosteatosis and dense subcutaneous fat) that were influential on reducing survival outcomes in this cohort. These features displayed a large degree of independence, and phenotypic overlap proved to be a further detriment to overall survival. Biological protein correlates were found in relation to each BC phenotype and ranged in function from inflammation to metabolic processes.

6.1 Body Composition Assessment in CRC

To our knowledge, this is the first study to examine the interdependence and subsequent influence of sarcopenia, myosteatosis and dense subcutaneous fat on overall survival outcomes

in a population of patients with CRC. Our work demonstrates that these phenotypes display a large degree of independence from one another (average of ~ 60 %). In addition, phenotypic overlap, especially of all three phenotypes, is particularly detrimental to OS. Typically in previous work BC phenotypes have been assessed as single measures, or at most have been examined two at a time (i.e. sarcopenia and myosteatosis) (32). It has been well-described that both sarcopenia and myosteatosis decrease overall survival outcomes in cancer populations, both when evaluated independently and simultaneously (32, 78). On the other hand, body compositions such as dense sub-q have only recently gained recognition to be clinically relevant and decrease survival outcomes in cancer populations (34). One group did evaluate the summative influence of sarcopenia, myosteatosis and visceral obesity in a cancer population comprised of 2100 pooled UK and Canadian cohort with CRC and found the concurrence of all three abnormal BC phenotypes was associated with worse clinical outcomes, such as longer length of hospital stays as well as more post-surgical complications when compared to patients with a lower number of body composition phenotypes (75). Our study, in supplement with this work, show that although body composition features can demonstrate a large degree of independence, it is also important to consider BC feature overlap, which may represent a more severely wasted individual (75). The examination of other detectable body compositions will continue to supplement models of cachectic wasting to give a better understanding of the mechanisms behind this syndrome.

6.2 Targeted Serum Proteomics

In order to assess biological mechanisms associated with each body feature we performed targeted serum proteomics on pre-operative samples of a subset of patients within our discovery cohort (N = 140). Proteins were selected based on functions previously described

in cancer settings as well as models of cachectic wasting (see Table 2.2, Chapter 2). In the myosteatosis phenotype we detected elevated concentrations of leptin, resistin and TNF-α and decreased IGF-1. To our knowledge, we are the first to detect such protein perturbations in CRC patients with myosteatosis. Myosteatosis is well-described in settings such as obesity, insulin resistance and aging; however, there is a rudimentary understanding of the myosteatosis phenotype in cancer settings (71, 178). Previous work has described myosteatosis in cancer settings as associated with upregulated inflammation. For instance, in CRC and pancreatic cancer patients that also had myosteatosis had elevated neutrophil-to-lymphocyte ratios, a measure for chronic inflammation (36, 77). This helps support the validity of our finding that the pro-inflammatory cytokine, TNF-α, was increased in our isolated myosteatosis phenotype. Other circulating features related to energy homeostasis were found to be perturbed in the patients with myosteatosis we well, which were increased leptin and resistin. Leptin is regarded as a pro-inflammatory adipokine, wherein animal models have revealed that exogenous supplementation of TNF-a results in elevations of leptin (51). Perhaps the observed increase in leptin in the myosteatosis phenotype is linked the pro-inflammatory cancer environment; however, leptin's role in energy homeostasis also suggests it may be promoting lipolysis, making the likelihood of ectopic fatty acid accumulation in tissues such as skeletal muscle more probable (125). In tandem with leptin, resistin was also observed in this phenotype which also has a role of increasing lipolysis in adipose tissue (129).

Inflammation may be involved in several of the etiological mechanisms of myosteatosis development. IGF-1 was also reduced in myosteatosis, which again may be linked to the inflammatory state of the host as decreased concentrations of IGF-1 have been documented in

cancer settings (57). Myosteatosis was also shown to be more prevalent in older patients, which may also help explain the reductions in IGF-1, where natural reductions in growth factors occur at older ages (179). Beyond myosteatosis, the dense sub-q phenotype was shown to be related to decreased concentrations of leptin. Dense sub-q fat is more commonly observed in individuals with reduced subcutaneous adipose tissue surface areas, which may be representative of a more "wasted" individual with reductions in adipose tissue reserves (75). This is also concurrent with work that has shown that cachectic individuals exhibit reductions in leptin, which may be what we are observing in this phenotype (180, 181). Overall, these findings provide support for continued investigation of body composition phenotypes in cancer settings, as circulating features suggest different mechanisms may be at play. A better understanding of the biology surrounding these features will provide an opportunity to improve interventions to mitigate cancer-associated tissue wasting.

6.3 Tumor Proteomics

To supplement the work performed on the sera proteomics, we conducted label-free shotgun proteomics on colorectal adenocarcinoma samples on a small cohort of male patients (N = 14) via LC-MS/MS analysis. Due to sample availability we limited our analyses to patients with isolated sarcopenia and isolated myosteatosis and compared them to the tumor proteomes of those with an absence of sarcopenia and myosteatosis. In our univariate analyses we were able to identify seven significantly perturbed proteins within the sarcopenia phenotype (compared to normal) and three within our myosteatosis compared to normal. These significant proteins participated in a wide array of functions, ranging from inflammation and metabolism to cell transport and histone involvement. In our multivariate analyses we identified 33 proteins

that were influential on differentiating the three phenotypes (Table 5.1, Chapter 5). Although several interesting hits were found, two important proteins were Latent TGF-B binding protein 4 (LTBP4) and ATP Binding Cassette Subfamily D Member 3 (ABCD3). Sarcopenia, for instance, had decreased abundance of the protein LTBP4, which is a protein that inhibits the action of TGF-beta (151). Interestingly, TGF-beta has been shown to perpetuate muscle atrophy in wasting models (170). On the other hand, myosteatosis was negatively associated with ABCD3, which transfers fatty acids from the cell cytosol to the peroxisome lumen in the mitochondria for beta-oxidation (138). This highlights the potential that patients with the myosteatosis may exhibit a reduction in beta-oxidative capacity (32, 138). Finally, we were also able to demonstrate, for the first time, that myosteatosis and sarcopenia can be distinctly separated from each other, as well from patients exhibiting no BC features, using multivariate analyses of data from the label-free proteomics experiment. Although this portion of the project was exploratory in nature, it certainly demonstrates the applicability and untapped potential that the use of proteomic technologies have in deepening our understanding of cancer-wasting mechanism through the identification of new, novel proteins.

6.4 Clinical Relevance

While the importance of cachexia on cancer patient outcomes continues to be recognized in the oncology community, further work is required to untangle the biological complexities surrounding this syndrome. More detailed measures of body composition analysis, such as CT assessment, have allowed for detailed quantification of fat and fat-free mass in ways that traditional measures of BC assessment, such as BMI, fall short (27). BC assessment via CT imaging allowed our study to highlight the importance of measuring body composition features beyond

that of low muscle mass (sarcopenia). Specifically, we demonstrate that both myosteatosis and dense sub-q are independent predictors of OS in our cohort of patients with CRC. We also demonstrate several protein perturbations associated with sarcopenia, myosteatosis and dense sub-q. These findings are important as they contribute to the understanding of tumor-mediated wasting and may inform the development of better therapeutics to such wasting. If muscle and adipose tissue loss could be limited, or even reversed, hopefully an improvement to quality of life, tolerance to treatments and survival outcomes would ensue.

Currently, there are limited treatment options for the management of cachexia as well as the body composition phenotypes that develop in tumor-mediated wasting (182). However, it is a common consensus in cachexia research that early detection and intervention is imperative to prevent patients from transitioning into the refractory stages of tissue wasting (20). The American Society of Clinical Oncology (ASCO) came out with guidelines for cachexia management, which discussed some potentially useful nutritional and pharmacological interventions. Each intervention strategy is ranked based on the strength of the recommendation (with associated evidence), as well as the benefits and harms of each (182).

A nutritional intervention with the highest recommendation is individualized dietary counselling with focus on adherence to a diet rich in high-protein/high-calorie nutrient dense foods (183-186). Evidence for pharmacological agents remain insufficient; however in cases of loss of appetite and weight loss, progesterone analogs (such as megestrol acetate) and corticosteroids can be offered, but are linked to edema and other toxicities (182, 187, 188). In regards to exercise intervention, the ASCO did not set any definitive guidelines. However, randomized control trials have revealed that cancer patient adherence to exercise regimes such

as resistance training, endurance training (with or without dietary supplementations) can improve muscle strength and maintain body mass (189). Certainly, further research is required to improve therapies to remediate tissue wasting, which will likely involve several avenues of intervention. Careful consideration of the different types of tissue wasting that can occur in cancer populations will hopefully improve the efficacy of intervention strategies.

6.5 Limitations and Future Directions

There are some limitations to address with this work. First, this is a retrospective cohort study, thereby this comes with the standard limitations of convenience sampling and the chance of misclassification biases. A chart review was performed for our cohort, but not all clinical factors (such as comorbidities) could be assessed which has the potential to introduce a confounding bias. We also can only comment on *associations* between body composition factors and our protein detections and not *causation*. Related to our experimental design, we did not control for contrast in our CT images, which has recently become more prevalent in body composition research. Targeted sera protein correlations between samples and CT images were only completed for samples with an absolute maximum date difference of 100 days. Ideally, we would have had our scans and blood draws closer together. Finally, our tumor proteomic experiments were certainly limited by our small sample size (N = 14) in addition to the inclusion of only male participants, which was due to a limitation of samples that met selection criteria.

With regards to future work in this project, we intend to examine the immune types of the tumors in each body composition phenotype group to determine if there is an association between CRC tumor development/etiology on BC development. In addition, we will assess the

neutrophil-to-lymphocyte ratio to quantify the level of inflammation in each BC phenotype. Finally, we also would like to perform more label-free tumor proteomic experiments on a greater number of CRC tumor samples, including both males and females, to strengthen and validate our preliminary findings on tumor proteome differences between the body composition phenotypic development.

Overall, this work is important as it demonstrates the complexity of tumor-mediated wasting. It shows that cancer wasting likely manifests as several body composition features that are detectable via CT scan and that the classical models of “cachexia” are currently overly simplistic and biased towards sarcopenia. Indeed, this work also demonstrates that biological differences in these three phenotypes do exist and are independent, and further work is needed to help delineate the mechanisms associated with these findings.

References

1. Sung H, Ferlay J, Siegel RL, Laversanne M, Soerjomataram I, Jemal A, et al. Global Cancer Statistics 2020: GLOBOCAN Estimates of Incidence and Mortality Worldwide for 36 Cancers in 185 Countries. CA: A Cancer Journal for Clinicians. 2021;71(3):209-49.
2. Henrikson NB, Webber EM, Goddard KA, Scrol A, Piper M, Williams MS, et al. Family history and the natural history of colorectal cancer: systematic review. Genet Med. 2015;17(9):702-12.
3. Syngal S, Brand RE, Church JM, Giardiello FM, Hampel HL, Burt RW. ACG clinical guideline: Genetic testing and management of hereditary gastrointestinal cancer syndromes. Am J Gastroenterol. 2015;110(2):223-62; quiz 63.
4. Jasperson KW, Tuohy TM, Neklason DW, Burt RW. Hereditary and Familial Colon Cancer. Gastroenterology. 2010;138(6):2044-58.
5. Mármol I, Sánchez-De-Diego C, Pradilla Dieste A, Cerrada E, Rodriguez Yoldi M. Colorectal Carcinoma: A General Overview and Future Perspectives in Colorectal Cancer. International Journal of Molecular Sciences. 2017;18(1):197.
6. Balchen V, Simon K. Colorectal cancer development and advances in screening. Clinical Interventions in Aging. 2016;Volume 11:967-76.
7. Dekker E, Tanis PJ, Vleugels JLA, Kasi PM, Wallace MB. Colorectal cancer. The Lancet. 2019;394(10207):1467-80.
8. Malki A, Elruz RA, Gupta I, Allouch A, Vranic S, Al Moustafa A-E. Molecular Mechanisms of Colon Cancer Progression and Metastasis: Recent Insights and Advancements. International Journal of Molecular Sciences. 2020;22(1):130.
9. Kang GH. Four molecular subtypes of colorectal cancer and their precursor lesions. Arch Pathol Lab Med. 2011;135(6):698-703.
10. Nojadeh JN, Behrouz Sharif S, Sakhinia E. Microsatellite instability in colorectal cancer. Excli j. 2018;17:159-68.
11. Kocarnik JM, Shiovitz S, Phipps AI. Molecular phenotypes of colorectal cancer and potential clinical applications. Gastroenterology Report. 2015:gov046.
12. Sun G, Wang S, Liu G. Preoperative neoadjuvant chemotherapy on surgical condition and oncogene expression in advanced gastric cancer. Pak J Med Sci. 2020;36(3):485-9.
13. Cameron MG, Kersten C, Vistad I, Fosså S, Guren MG. Palliative pelvic radiotherapy of symptomatic incurable rectal cancer - a systematic review. Acta Oncol. 2014;53(2):164-73.
14. Best L, Simmonds P, Baughan C, Buchanan R, Davis C, Fentiman I, et al. Palliative chemotherapy for advanced or metastatic colorectal cancer. Colorectal Meta-analysis Collaboration. Cochrane Database Syst Rev. 2000;2000(2):Cd001545.
15. Wolpin BM, Mayer RJ. Systemic Treatment of Colorectal Cancer. Gastroenterology. 2008;134(5):1296-310.e1.
16. Ferrara N, Hillan KJ, Novotny W. Bevacizumab (Avastin), a humanized anti-VEGF monoclonal antibody for cancer therapy. Biochem Biophys Res Commun. 2005;333(2):328-35.
17. Kong JC, Soucisse M, Michael M, Tie J, Ngan SY, Leong T, et al. Total Neoadjuvant Therapy in Locally Advanced Rectal Cancer: A Systematic Review and Metaanalysis of Oncological and Operative Outcomes. Annals of Surgical Oncology. 2021;28(12):7476-86.
18. Housman G, Byler S, Heerboth S, Lapinska K, Longacre M, Snyder N, et al. Drug resistance in cancer: an overview. Cancers (Basel). 2014;6(3):1769-92.
19. Pin F, Barreto R, Couch ME, Bonetto A, O'Connell TM. Cachexia induced by cancer and chemotherapy yield distinct perturbations to energy metabolism. Journal of Cachexia, Sarcopenia and Muscle. 2019;10(1):140-54.

20. Fearon K, Strasser F, Anker SD, Bosaeus I, Bruera E, Fainsinger RL, et al. Definition and classification of cancer cachexia: an international consensus. The Lancet Oncology. 2011;12(5):489-95.
21. Le Bricon T, Gugins S, Cynober L, Baracos VE. Negative impact of cancer chemotherapy on protein metabolism in healthy and tumor-bearing rats. Metabolism. 1995;44(10):1340-8.
22. Barreto R, Waning DL, Gao H, Liu Y, Zimmers TA, Bonetto A. Chemotherapy-related cachexia is associated with mitochondrial depletion and the activation of ERK1/2 and p38 MAPKs. Oncotarget. 2016;7(28):43442-60.
23. Porporato PE. Understanding cachexia as a cancer metabolism syndrome. Oncogenesis. 2016;5(2):e200-e.
24. Tisdale MJ. Mechanisms of cancer cachexia. Physiol Rev. 2009;89(2):381-410.
25. García-Figueiras R, Baleato-González S, Canedo-Antelo M, Alcalá L, Marhuenda A. Imaging Advances on CT and MRI in Colorectal Cancer. Current Colorectal Cancer Reports. 2021;17(6):113-30.
26. Baracos VE, Mazurak VC, Bhullar AS. Cancer cachexia is defined by an ongoing loss of skeletal muscle mass. Ann Palliat Med. 2019;8(1):3-12.
27. Tolonen A, Pakarinen T, Sassi A, Kyttä J, Cancino W, Rinta-Kiikka I, et al. Methodology, clinical applications, and future directions of body composition analysis using computed tomography (CT) images: A review. European Journal of Radiology. 2021;145:109943.
28. Aubrey J, Esfandiari N, Baracos VE, Buteau FA, Frenette J, Putman CT, et al. Measurement of skeletal muscle radiation attenuation and basis of its biological variation. Acta Physiologica. 2014;210(3):489-97.
29. Morsbach F, Zhang YH, Martin L, Lindqvist C, Brismar T. Body composition evaluation with computed tomography: Contrast media and slice thickness cause methodological errors. Nutrition. 2019;59:50-5.
30. Shachar SS, Williams GR, Muss HB, Nishijima TF. Prognostic value of sarcopenia in adults with solid tumours: A meta-analysis and systematic review. Eur J Cancer. 2016;57:58-67.
31. Chindapasirt J. Sarcopenia in Cancer Patients. Asian Pac J Cancer Prev. 2015;16(18):8075-7.
32. Stretch C, Aubin J-M, Mickiewicz B, Leugner D, Al-Manasra T, Tobola E, et al. Sarcopenia and myosteatosis are accompanied by distinct biological profiles in patients with pancreatic and periampullary adenocarcinomas. PLOS ONE. 2018;13(5):e0196235.
33. Feliciano EMC, Winkels RM, Meyerhardt JA, Prado CM, Afman LA, Caan BJ. Abdominal adipose tissue radiodensity is associated with survival after colorectal cancer. The American Journal of Clinical Nutrition. 2021;114(6):1917-24.
34. Charette N, Vandeputte C, Ameye L, Bogaert CV, Krygier J, Guiot T, et al. Prognostic value of adipose tissue and muscle mass in advanced colorectal cancer: a post hoc analysis of two non-randomized phase II trials. BMC Cancer. 2019;19(1):134.
35. Mizuno S, Seishima R, Okabayashi K, Shigeta K, Matsui S, Kitagawa Y. Sarcopenic obesity is a postoperative prognostic factor for stage II and III colorectal cancer. Journal of Gastrointestinal Surgery. 2021;25(11):2951-3.
36. Rollins KE, Tewari N, Ackner A, Awwad A, Madhusudan S, Macdonald IA, et al. The impact of sarcopenia and myosteatosis on outcomes of unresectable pancreatic cancer or distal cholangiocarcinoma. Clin Nutr. 2016;35(5):1103-9.
37. Prado CMMB, Lieffers JRRD, McCargar LJP, Reiman TMD, Sawyer MBMD, Martin LM, et al. Prevalence and clinical implications of sarcopenic obesity in patients with solid tumours of the respiratory and gastrointestinal tracts: a population-based study. Lancet Oncol. 2008;9(7):629-35.
38. Poulia KA, Sarantis P, Antoniadou D, Koustas E, Papadimitropoulou A, Papavassiliou AG, et al. Pancreatic Cancer and Cachexia-Metabolic Mechanisms and Novel Insights. Nutrients. 2020;12(6):1543.
39. Argilés JM, Busquets S, Stemmler B, López-Soriano FJ. Cancer cachexia: understanding the molecular basis. Nat Rev Cancer. 2014;14(11):754-62.

40. Armstrong VS, Fitzgerald LW, Bathe OF. Cancer-Associated Muscle Wasting-Candidate Mechanisms and Molecular Pathways. Int J Mol Sci. 2020;21(23).
41. Feliciano EMC, Kroenke CH, Meyerhardt JA, Prado CM, Bradshaw PT, Kwan ML, et al. Association of Systemic Inflammation and Sarcopenia With Survival in Nonmetastatic Colorectal Cancer: Results From the C SCANS Study. JAMA Oncol. 2017;3(12):e172319.
42. Hanahan D, Robert. Hallmarks of Cancer: The Next Generation. Cell. 2011;144(5):646-74.
43. Ma JF, Sanchez BJ, Hall DT, Tremblay AK, Di Marco S, Gallouzi IE. STAT3 promotes IFNγ/TNFα-induced muscle wasting in an NF-κB-dependent and IL-6-independent manner. EMBO Mol Med. 2017;9(5):622-37.
44. Volanakis JE. Human C-reactive protein: expression, structure, and function. Mol Immunol. 2001;38(2-3):189-97.
45. Okugawa Y, Toiyama Y, Yamamoto A, Shigemori T, Kitamura A, Ichikawa T, et al. Close Relationship Between Immunological/Inflammatory Markers and Myopenia and Myosteatosis in Patients With Colorectal Cancer: A Propensity Score Matching Analysis. JPEN J Parenter Enteral Nutr. 2019;43(4):508-15.
46. Baracos VE, Martin L, Korc M, Guttridge DC, Fearon KCH. Cancer-associated cachexia. Nature Reviews Disease Primers. 2018;4(1):17105.
47. Langen RC, Van Der Velden JL, Schols AM, Kelders MC, Wouters EF, Janssen-Heininger YM. Tumor necrosis factor-alpha inhibits myogenic differentiation through MyoD protein destabilization. Faseb j. 2004;18(2):227-37.
48. Baazim H, Antonio-Herrera L, Bergthaler A. The interplay of immunology and cachexia in infection and cancer. Nature Reviews Immunology. 2021.
49. Braun TP, Zhu X, Szumowski M, Scott GD, Grossberg AJ, Levasseur PR, et al. Central nervous system inflammation induces muscle atrophy via activation of the hypothalamic-pituitary-adrenal axis. J Exp Med. 2011;208(12):2449-63.
50. Braun TP, Marks DL. The regulation of muscle mass by endogenous glucocorticoids. Frontiers in physiology. 2015;6:12-.
51. Engineer DR, Garcia JM. Leptin in anorexia and cachexia syndrome. Int J Pept. 2012;2012:287457.
52. Bonaldo P, Sandri M. Cellular and molecular mechanisms of muscle atrophy. Dis Model Mech. 2013;6(1):25-39.
53. Cohen S, Nathan JA, Goldberg AL. Muscle wasting in disease: molecular mechanisms and promising therapies. Nat Rev Drug Discov. 2015;14(1):58-74.
54. Tisdale MJ. Protein Metabolism in Cachexia. Springer Milan. p. 185-90.
55. Schiaffino S, Mammucari C. Regulation of skeletal muscle growth by the IGF1-Akt/PKB pathway: insights from genetic models. Skeletal Muscle. 2011;1(1):4.
56. Miyamoto Y, Hanna DL, Zhang W, Baba H, Lenz H-J. Molecular Pathways: Cachexia Signaling—A Targeted Approach to Cancer Treatment. Clinical Cancer Research. 2016;22(16):3999-4004.
57. Vanhorebeek I, Van den Berghe G. The neuroendocrine response to critical illness is a dynamic process. Crit Care Clin. 2006;22(1):1-15, v.
58. Huang XY, Huang ZL, Yang JH, Xu YH, Sun JS, Zheng Q, et al. Pancreatic cancer cell-derived IGFBP-3 contributes to muscle wasting. J Exp Clin Cancer Res. 2016;35:46.
59. Cole CL, Bachman JF, Ye J, Murphy J, Gerber SA, Beck CA, et al. Increased myocellular lipid and IGFBP-3 expression in a pre-clinical model of pancreatic cancer-related skeletal muscle wasting. Journal of Cachexia, Sarcopenia and Muscle. 2021;12(3):731-45.
60. Cole CL, Kleckner IR, Jatoi A, Schwarz E, Dunne RF. The Role of Systemic Inflammation in Cancer-Associated Muscle Wasting and Rationale for Exercise as a Therapeutic Intervention. JCSM Clinical Reports. 2018;3(2).

61. Dogra C, Changotra H, Mohan S, Kumar A. Tumor Necrosis Factor-like Weak Inducer of Apoptosis Inhibits Skeletal Myogenesis through Sustained Activation of Nuclear Factor-κB and Degradation of MyoD Protein*. Journal of Biological Chemistry. 2006;281(15):10327-36.
62. Trendelenburg AU, Meyer A, Rohner D, Boyle J, Hatakeyama S, Glass DJ. Myostatin reduces Akt/TORC1/p70S6K signaling, inhibiting myoblast differentiation and myotube size. Am J Physiol Cell Physiol. 2009;296(6):C1258-70.
63. Bodine SC, Baehr LM. Skeletal muscle atrophy and the E3 ubiquitin ligases MuRF1 and MAFbx/atrogin-1. Am J Physiol Endocrinol Metab. 2014;307(6):E469-84.
64. Adams V, Mangner N, Gasch A, Krohne C, Gielen S, Hirner S, et al. Induction of MuRF1 is essential for TNF-alpha-induced loss of muscle function in mice. J Mol Biol. 2008;384(1):48-59.
65. McFarlane C, Plummer E, Thomas M, Hennebry A, Ashby M, Ling N, et al. Myostatin induces cachexia by activating the ubiquitin proteolytic system through an NF-kappaB-independent, FoxO1-dependent mechanism. J Cell Physiol. 2006;209(2):501-14.
66. Pettersen K, Andersen S, Degen S, Tadini V, Grosjean J, Hatakeyama S, et al. Cancer cachexia associates with a systemic autophagy-inducing activity mimicked by cancer cell-derived IL-6 trans-signaling. Sci Rep. 2017;7(1):2046.
67. Penna F, Costamagna D, Pin F, Camperi A, Fanzani A, Chiarpotto EM, et al. Autophagic Degradation Contributes to Muscle Wasting in Cancer Cachexia. The American Journal of Pathology. 2013;182(4):1367-78.
68. Aleixo GFP, Shachar SS, Nyrop KA, Muss HB, Malpica L, Williams GR. Myosteatosis and prognosis in cancer: Systematic review and meta-analysis. Crit Rev Oncol Hematol. 2020;145:102839.
69. Armstrong V, Stretch C, Fitzgerald L, Gopaul A, McKinnon G, Koziak J, et al. Characterizing cancer-associated myosteatosis: anatomic distribution and cancer-specific variability of low radiodensity muscle. JCSM Rapid Communications. 2021;4(2):197-206.
70. Correa-de-Araujo R, Addison O, Miljkovic I, Goodpaster BH, Bergman BC, Clark RV, et al. Myosteatosis in the Context of Skeletal Muscle Function Deficit: An Interdisciplinary Workshop at the National Institute on Aging. Frontiers in Physiology. 2020;11.
71. Goodpaster BH, Thaete FL, Kelley DE. Thigh adipose tissue distribution is associated with insulin resistance in obesity and in type 2 diabetes mellitus. Am J Clin Nutr. 2000;71(4):885-92.
72. Hopkins JJ, Reif RL, Bigam DL, Baracos VE, Eurich DT, Sawyer MB. The Impact of Muscle and Adipose Tissue on Long-term Survival in Patients With Stage I to III Colorectal Cancer. Dis Colon Rectum. 2019;62(5):549-60.
73. Aro R, Mäkäräinen-Uhlbäck E, Ämmälä N, Rautio T, Ohtonen P, Saarnio J, et al. The impact of sarcopenia and myosteatosis on postoperative outcomes and 5-year survival in curatively operated colorectal cancer patients - A retrospective register study. Eur J Surg Oncol. 2020;46(9):1656-62.
74. Martin L, Gioulbasanis I, Senesse P, Baracos VE. Cancer-Associated Malnutrition and CT-Defined Sarcopenia and Myosteatosis Are Endemic in Overweight and Obese Patients. JPEN J Parenter Enteral Nutr. 2020;44(2):227-38.
75. Martin L, Hopkins J, Malietzis G, Jenkins JT, Sawyer MB, Brisebois R, et al. Assessment of Computed Tomography (CT)-Defined Muscle and Adipose Tissue Features in Relation to Short-Term Outcomes After Elective Surgery for Colorectal Cancer: A Multicenter Approach. Annals of Surgical Oncology. 2018;25(9):2669-80.
76. Wilson HE, Stanton DA, Rellick S, Geldenhuys W, Pistilli EE. Breast cancer-associated skeletal muscle mitochondrial dysfunction and lipid accumulation is reversed by PPARG. American journal of physiology Cell physiology. 2021;320(4):C577-C90.
77. Malietzis G, Johns N, Al-Hassi HO, Knight SC, Kennedy RH, Fearon KC, et al. Low Muscularity and Myosteatosis Is Related to the Host Systemic Inflammatory Response in Patients Undergoing Surgery for Colorectal Cancer. Ann Surg. 2016;263(2):320-5.

78. Dolan RD, Almasaudi AS, Dieu LB, Horgan PG, McSorley ST, McMillan DC. The relationship between computed tomography-derived body composition, systemic inflammatory response, and survival in patients undergoing surgery for colorectal cancer. J Cachexia Sarcopenia Muscle. 2019;10(1):111-22.
79. Miljkovic I, Kuipers AL, Kammerer CM, Wang X, Bunker CH, Patrick AL, et al. Markers of inflammation are heritable and associated with subcutaneous and ectopic skeletal muscle adiposity in African ancestry families. Metab Syndr Relat Disord. 2011;9(4):319-26.
80. Van Hollebeke RB, Cushman M, Schlueter EF, Allison MA. Abdominal Muscle Density Is Inversely Related to Adiposity Inflammatory Mediators. Medicine & Science in Sports & Exercise. 2018;50(7):1495-501.
81. Vella CA, Allison MA. Associations of abdominal intermuscular adipose tissue and inflammation: The Multi-Ethnic Study of Atherosclerosis. Obes Res Clin Pract. 2018;12(6):534-40.
82. Cawthorn WP, Sethi JK. TNF-alpha and adipocyte biology. FEBS Lett. 2008;582(1):117-31.
83. Montgomery MK, Nardo WD, Watt MJ. Impact of Lipotoxicity on Tissue “Cross Talk” and Metabolic Regulation. Physiology. 2019;34(2):134-49.
84. Lee S-H, Park S-Y, Choi CS. Insulin Resistance: From Mechanisms to Therapeutic Strategies. Diabetes & Metabolism Journal. 2022;46(1):15-37.
85. Miljkovic I, Vella CA, Allison M. Computed Tomography-Derived Myosteatosis and Metabolic Disorders. Diabetes & Metabolism Journal. 2021;45(4):482-91.
86. Anciaux M, Van Gossum A, Wenglinski C, Ameye L, Guiot T, Flamen P, et al. Fat density is a novel prognostic marker in patients with esophageal cancer. Clin Nutr ESPEN. 2020;39:124-30.
87. Gregoire FM, Smas CM, Sul HS. Understanding adipocyte differentiation. Physiol Rev. 1998;78(3):783-809.
88. Petruzzelli M, Schweiger M, Schreiber R, Campos-Olivas R, Tsoli M, Allen J, et al. A switch from white to brown fat increases energy expenditure in cancer-associated cachexia. Cell Metab. 2014;20(3):433-47.
89. Kir S, White JP, Kleiner S, Kazak L, Cohen P, Baracos VE, et al. Tumour-derived PTH-related protein triggers adipose tissue browning and cancer cachexia. Nature. 2014;513(7516):100-4.
90. Shen W, Punyanitya M, Wang Z, Gallagher D, St.-Onge M-P, Albu J, et al. Total body skeletal muscle and adipose tissue volumes: estimation from a single abdominal cross-sectional image. Journal of Applied Physiology. 2004;97(6):2333-8.
91. Martin L, Birdsell L, MacDonald N, Reiman T, Clandinin MT, McCargar LJ, et al. Cancer Cachexia in the Age of Obesity: Skeletal Muscle Depletion Is a Powerful Prognostic Factor, Independent of Body Mass Index. Journal of Clinical Oncology. 2013;31(12):1539-47.
92. Ogłuszka M, Orzechowska M, Jędroszka D, Witas P, Bednarek AK. Evaluate Cutpoints: Adaptable continuous data distribution system for determining survival in Kaplan-Meier estimator. Computer Methods and Programs in Biomedicine. 2019;177:133-9.
93. Gray S, Axelsson B. The prevalence of deranged C-reactive protein and albumin in patients with incurable cancer approaching death. PLoS One. 2018;13(3):e0193693.
94. Patel HJ, Patel BM. TNF-α and cancer cachexia: Molecular insights and clinical implications. Life Sci. 2017;170:56-63.
95. Soumoy L, Kindt N, Ghanem G, Saussez S, Journe F. Role of Macrophage Migration Inhibitory Factor (MIF) in Melanoma. Cancers. 2019;11(4):529.
96. Kubala MH, Punj V, Placencio-Hickok VR, Fang H, Fernandez GE, Sposto R, et al. Plasminogen Activator Inhibitor-1 Promotes the Recruitment and Polarization of Macrophages in Cancer. Cell Rep. 2018;25(8):2177-91.e7.

97. Rebalka IA, Monaco CMF, Varah NE, Berger T, D'Souza D M, Zhou S, et al. Loss of the adipokine lipocalin-2 impairs satellite cell activation and skeletal muscle regeneration. Am J Physiol Cell Physiol. 2018;315(5):C714-c21.
98. Danese E, Montagnana M, Minicozzi AM, Bonafini S, Ruzzenente O, Gelati M, et al. The role of resistin in colorectal cancer. Clin Chim Acta. 2012;413(7-8):760-4.
99. Sin TK, Zhang G, Zhang Z, Gao S, Li M, Li YP. Cancer Takes a Toll on Skeletal Muscle by Releasing Heat Shock Proteins-An Emerging Mechanism of Cancer-Induced Cachexia. Cancers (Basel). 2019;11(9).
100. Morley JE, Thomas DR, Wilson M-MG. Cachexia: pathophysiology and clinical relevance. The American Journal of Clinical Nutrition. 2006;83(4):735-43.
101. Penna F, Camperi A, Muscaritoli M, Filigheddu N, Costelli P. The role of vitamin D in cancer cachexia. Current Opinion in Supportive and Palliative Care. 2017;11(4):287-92.
102. Morley JE, Thomas DR, Wilson MM. Cachexia: pathophysiology and clinical relevance. Am J Clin Nutr. 2006;83(4):735-43.
103. Wolf I, Sadetzki S, Kanety H, Kundel Y, Pariente C, Epstein N, et al. Adiponectin, ghrelin, and leptin in cancer cachexia in breast and colon cancer patients. Cancer. 2006;106(4):966-73.
104. Trobec K, von Haehling S, Anker SD, Lainscak M. Growth hormone, insulin-like growth factor 1, and insulin signaling-a pharmacological target in body wasting and cachexia. J Cachexia Sarcopenia Muscle. 2011;2(4):191-200.
105. Liu M, Liu F. Regulation of adiponectin multimerization, signaling and function. Best Pract Res Clin Endocrinol Metab. 2014;28(1):25-31.
106. Song NJ, Kim S, Jang BH, Chang SH, Yun UJ, Park KM, et al. Small Molecule-Induced Complement Factor D (Adipsin) Promotes Lipid Accumulation and Adipocyte Differentiation. PLoS One. 2016;11(9):e0162228.
107. Petruzzelli M, Wagner EF. Mechanisms of metabolic dysfunction in cancer-associated cachexia. Genes Dev. 2016;30(5):489-501.
108. Baccam A, Benoni-Sviercovich A, Rocchi M, Moresi V, Seelaender M, Li Z, et al. The Mechanical Stimulation of Myotubes Counteracts the Effects of Tumor-Derived Factors Through the Modulation of the Activin/Follistatin Ratio. Front Physiol. 2019;10:401.
109. Wright TJ, Dillon EL, Durham WJ, Chamberlain A, Randolph KM, Danesi C, et al. A randomized trial of adjunct testosterone for cancer-related muscle loss in men and women. J Cachexia Sarcopenia Muscle. 2018;9(3):482-96.
110. Elshal MF, McCoy JP. Multiplex bead array assays: performance evaluation and comparison of sensitivity to ELISA. Methods. 2006;38(4):317-23.
111. Consortium TU. UniProt: the universal protein knowledgebase in 2021. Nucleic Acids Research. 2020;49(D1):D480-D9.
112. Sato R, Oikawa M, Kakita T, Okada T, Abe T, Yazawa T, et al. Impact of Sarcopenia on Postoperative Complications in Obstructive Colorectal Cancer Patients Who Received Stenting as a Bridge to Curative Surgery. J Anus Rectum Colon. 2022;6(1):40-51.
113. Shirdel M, Andersson F, Myte R, Axelsson J, Rutegård M, Blomqvist L, et al. Body composition measured by computed tomography is associated with colorectal cancer survival, also in early-stage disease. Acta Oncol. 2020;59(7):799-808.
114. McSorley ST, Black DH, Horgan PG, McMillan DC. The relationship between tumour stage, systemic inflammation, body composition and survival in patients with colorectal cancer. Clin Nutr. 2018;37(4):1279-85.
115. Xiao J, Caan BJ, Elizabeth M, Meyerhardt JA, Kroenke CH, Baracos VE, et al. The association of medical and demographic characteristics with sarcopenia and low muscle radiodensity in patients with nonmetastatic colorectal cancer. The American Journal of Clinical Nutrition. 2019;109(3):615-25.

116. Côté JA, Nazare JA, Nadeau M, Leboeuf M, Blackburn L, Després JP, et al. Computed tomography-measured adipose tissue attenuation and area both predict adipocyte size and cardiometabolic risk in women. Adipocyte. 2016;5(1):35-42.
117. Patlas MP, J. Mourtzakis, M. Computed Tomography (CT) Assessment of Visceral Adiposity. OMICS Journal of Radiology. 2012.
118. Potretzke AM, Schmitz KH, Jensen MD. Preventing Overestimation of Pixels in Computed Tomography Assessment of Visceral Fat. Obesity Research. 2004;12(10):1698-701.
119. Lohmann AE, Dowling RJO, Ennis M, Amir E, Elser C, Brezden-Masley C, et al. Association of Metabolic, Inflammatory, and Tumor Markers With Circulating Tumor Cells in Metastatic Breast Cancer. JNCI Cancer Spectrum. 2018;2(2).
120. Li YP, Reid MB. NF-kappaB mediates the protein loss induced by TNF-alpha in differentiated skeletal muscle myotubes. Am J Physiol Regul Integr Comp Physiol. 2000;279(4):R1165-70.
121. Ma JF, Sanchez BJ, Hall DT, Tremblay A-MK, Di Marco S, Gallouzi I-E. STAT3 promotes IFNγ/TNFα-induced muscle wasting in an NF-κB-dependent and IL-6-independent manner. EMBO Mol Med. 2017;9(5):622-37.
122. Tavares P, Gonçalves DM, Santos LL, Ferreira R. Revisiting the clinical usefulness of C-reactive protein in the set of cancer cachexia. Porto Biomed J. 2021;6(1):e123-e.
123. Turpin SM, Ryall JG, Southgate R, Darby I, Hevener AL, Febbraio MA, et al. Examination of 'lipotoxicity' in skeletal muscle of high-fat fed andob/obmice. The Journal of Physiology. 2009;587(7):1593-605.
124. Pereira S, Cline DL, Glavas MM, Covey SD, Kieffer TJ. Tissue-Specific Effects of Leptin on Glucose and Lipid Metabolism. Endocrine Reviews. 2021;42(1):1-28.
125. Harris RBS. Direct and indirect effects of leptin on adipocyte metabolism. Biochimica et Biophysica Acta (BBA) - Molecular Basis of Disease. 2014;1842(3):414-23.
126. Chen N, Zhou L, Zhang Z, Xu J, Wan Z, Qin L. Resistin induces lipolysis and suppresses adiponectin secretion in cultured human visceral adipose tissue. Regul Pept. 2014;194-195:49-54.
127. Lo Iacono M, Modica C, Porcelli G, Brancato OR, Muratore G, Bianca P, et al. Targeting of the Peritumoral Adipose Tissue Microenvironment as an Innovative Antitumor Therapeutic Strategy. Biomolecules. 2022;12(5):702.
128. Iikuni N, Lam QLK, Lu L, Matarese G, La Cava A. Leptin and Inflammation. Curr Immunol Rev. 2008;4(2):70-9.
129. Su K-z, Li Y-r, Zhang D, Yuan J-h, Zhang C-s, Liu Y, et al. Relation of Circulating Resistin to Insulin Resistance in Type 2 Diabetes and Obesity: A Systematic Review and Meta-Analysis. Frontiers in Physiology. 2019;10.
130. Deng M, Vaes RDW, Van Bijnen AAJHM, Olde Damink SWM, Rensen SS. Activation of the Complement System in Patients with Cancer Cachexia. Cancers. 2021;13(22):5767.
131. Lubbers R, van Essen MF, van Kooten C, Trouw LA. Production of complement components by cells of the immune system. Clin Exp Immunol. 2017;188(2):183-94.
132. Fielitz J. Cancer cachexia—when proteasomal inhibition is not enough. Journal of Cachexia, Sarcopenia and Muscle. 2016;7(3):239-45.
133. Zhang G, Liu Z, Ding H, Zhou Y, Doan HA, Sin KWT, et al. Tumor induces muscle wasting in mice through releasing extracellular Hsp70 and Hsp90. Nat Commun. 2017;8(1):589.
134. Zhou X, Wang JL, Lu J, Song Y, Kwak KS, Jiao Q, et al. Reversal of cancer cachexia and muscle wasting by ActRIIB antagonism leads to prolonged survival. Cell. 2010;142(4):531-43.
135. Pettersen K, Andersen S, van der Veen A, Nonstad U, Hatakeyama S, Lambert C, et al. Autocrine activin A signalling in ovarian cancer cells regulates secretion of interleukin 6, autophagy, and cachexia. J Cachexia Sarcopenia Muscle. 2020;11(1):195-207.

136. Seto DN, Kandarian SC, Jackman RW. A Key Role for Leukemia Inhibitory Factor in C26 Cancer Cachexia. J Biol Chem. 2015;290(32):19976-86.
137. Kwon YW, Jo H-S, Bae S, Seo Y, Song P, Song M, et al. Application of Proteomics in Cancer: Recent Trends and Approaches for Biomarkers Discovery. Frontiers in Medicine. 2021;8.
138. van Roermund CW, Ijlst L, Wagemans T, Wanders RJ, Waterham HR. A role for the human peroxisomal half-transporter ABCD3 in the oxidation of dicarboxylic acids. Biochim Biophys Acta. 2014;1841(4):563-8.
139. Ensenauer R, He M, Willard JM, Goetzman ES, Corydon TJ, Vandahl BB, et al. Human acyl-CoA dehydrogenase-9 plays a novel role in the mitochondrial beta-oxidation of unsaturated fatty acids. J Biol Chem. 2005;280(37):32309-16.
140. Dzeja PP, Chung S, Terzic A. Integration of Adenylate Kinase and Glycolytic and Glycogenolytic Circuits in Cellular Energetics. Molecular System Bioenergetics2007. p. 265-301.
141. Xu T, Pagadala V, Mueller DM. Understanding structure, function, and mutations in the mitochondrial ATP synthase. Microb Cell. 2015;2(4):105-25.
142. Corduan A, Lecomte S, Martin C, Michel D, Desmots F. Sequential interplay between BAG6 and HSP70 upon heat shock. Cell Mol Life Sci. 2009;66(11-12):1998-2004.
143. Chai J, Du C, Wu JW, Kyin S, Wang X, Shi Y. Structural and biochemical basis of apoptotic activation by Smac/DIABLO. Nature. 2000;406(6798):855-62.
144. Casper JM, Kemp MG, Ghosh M, Randall GM, Vaillant A, Leffak M. The c-myc DNA-unwinding element-binding protein modulates the assembly of DNA replication complexes in vitro. J Biol Chem. 2005;280(13):13071-83.
145. He Z, Yang J, Sui C, Zhang P, Wang T, Mou T, et al. FAM98A promotes resistance to 5-fluorouracil in colorectal cancer by suppressing ferroptosis. Arch Biochem Biophys. 2022;722:109216.
146. Ai Y, Basu M, Bergsma DJ, Stambolian D. Comparison of the enzymatic activities of human galactokinase GALK1 and a related human galactokinase protein GK2. Biochem Biophys Res Commun. 1995;212(2):687-91.
147. Nass N, Brömme H-J, Hartig R, Korkmaz S, Sel S, Hirche F, et al. Differential response to α-oxoaldehydes in tamoxifen resistant MCF-7 breast cancer cells. PloS one. 2014;9(7):e101473-e.
148. Huang Y, Huang S, Ma L, Wang Y, Wang X, Xiao L, et al. Exploring the Prognostic Value, Immune Implication and Biological Function of H2AFY Gene in Hepatocellular Carcinoma. Front Immunol. 2021;12:723293.
149. Li JY, Patterson M, Mikkola HK, Lowry WE, Kurdistani SK. Dynamic distribution of linker histone H1.5 in cellular differentiation. PLoS Genet. 2012;8(8):e1002879.
150. Tagami H, Ray-Gallet D, Almouzni G, Nakatani Y. Histone H3.1 and H3.3 complexes mediate nucleosome assembly pathways dependent or independent of DNA synthesis. Cell. 2004;116(1):51-61.
151. Heydemann A, Ceco E, Lim JE, Hadhazy M, Ryder P, Moran JL, et al. Latent TGF-β–binding protein 4 modifies muscular dystrophy in mice. Journal of Clinical Investigation. 2009;119(12):3703-12.
152. Schmidt M, Poser C, von Maltzahn J. Wnt7a Counteracts Cancer Cachexia. Molecular Therapy - Oncolytics. 2020;16:134-46.
153. Lee KS, Kwak Y, Nam KH, Kim D-W, Kang S-B, Choe G, et al. Favorable prognosis in colorectal cancer patients with co-expression of c-MYC and ß-catenin. BMC Cancer. 2016;16(1).
154. Cazzalini O, Sommatis S, Tillhon M, Dutto I, Bachi A, Rapp A, et al. CBP and p300 acetylate PCNA to link its degradation with nucleotide excision repair synthesis. Nucleic Acids Res. 2014;42(13):8433-48.
155. Wang DG, Paddock MN, Lundquist MR, Sun JY, Mashadova O, Amadiume S, et al. PIP4Ks Suppress Insulin Signaling through a Catalytic-Independent Mechanism. Cell Rep. 2019;27(7):1991-2001.e5.

156. Jobling RK, Assoum M, Gakh O, Blaser S, Raiman JA, Mignot C, et al. PMPCA mutations cause abnormal mitochondrial protein processing in patients with non-progressive cerebellar ataxia. Brain. 2015;138(Pt 6):1505-17.
157. Kanayama HO, Tamura T, Ugai S, Kagawa S, Tanahashi N, Yoshimura T, et al. Demonstration that a human 26S proteolytic complex consists of a proteasome and multiple associated protein components and hydrolyzes ATP and ubiquitin-ligated proteins by closely linked mechanisms. Eur J Biochem. 1992;206(2):567-78.
158. Zhang L, Zhang X, Hsieh LS, Lin TV, Bordey A. Rab27a-Dependent Paracrine Communication Controls Dendritic Spine Formation and Sensory Responses in the Barrel Cortex. Cells. 2021;10(3).
159. Zhang Y, You J, Wang X, Weber J. The DHX33 RNA Helicase Promotes mRNA Translation Initiation. Mol Cell Biol. 2015;35(17):2918-31.
160. Hoshino A, Wang W-J, Wada S, McDermott-Roe C, Evans CS, Gosis B, et al. The ADP/ATP translocase drives mitophagy independent of nucleotide exchange. Nature. 2019;575(7782):375-9.
161. Reisman D, Glaros S, Thompson EA. The SWI/SNF complex and cancer. Oncogene. 2009;28(14):1653-68.
162. McCormack NM, Villalón E, Viollet C, Soltis AR, Dalgard CL, Lorson CL, et al. Survival motor neuron deficiency slows myoblast fusion through reduced myomaker and myomixer expression. Journal of cachexia, sarcopenia and muscle. 2021;12(4):1098-116.
163. Gaudet P, Livstone MS, Lewis SE, Thomas PD. Phylogenetic-based propagation of functional annotations within the Gene Ontology consortium. Brief Bioinform. 2011;12(5):449-62.
164. Putker M, Madl T, Vos HR, de Ruiter H, Visscher M, van den Berg MC, et al. Redox-dependent control of FOXO/DAF-16 by transportin-1. Mol Cell. 2013;49(4):730-42.
165. Thakurdas SM, Melicoff E, Sansores-Garcia L, Moreira DC, Petrova Y, Stevens RL, et al. The mast cell-restricted tryptase mMCP-6 has a critical immunoprotective role in bacterial infections. J Biol Chem. 2007;282(29):20809-15.
166. Mayans O, van der Ven PF, Wilm M, Mues A, Young P, Fürst DO, et al. Structural basis for activation of the titin kinase domain during myofibrillogenesis. Nature. 1998;395(6705):863-9.
167. Allen S, Abuzenadah AM, Hinks J, Blagg JL, Gursel T, Ingerslev J, et al. A novel von Willebrand disease-causing mutation (Arg273Trp) in the von Willebrand factor propeptide that results in defective multimerization and secretion. Blood. 2000;96(2):560-8.
168. Martínez-Hernández PL, Hernanz-Macías Á, Gómez-Candela C, Grande-Aragón C, Feliu-Batlle J, Castro-Carpeño J, et al. Serum interleukin-15 levels in cancer patients with cachexia. Oncol Rep. 2012;28(4):1443-52.
169. Mingot JM, Bohnsack MT, Jäkle U, Görlich D. Exportin 7 defines a novel general nuclear export pathway. Embo j. 2004;23(16):3227-36.
170. Mendias CL, Gumucio JP, Davis ME, Bromley CW, Davis CS, Brooks SV. Transforming growth factor-beta induces skeletal muscle atrophy and fibrosis through the induction of atrogin-1 and scleraxis. Muscle Nerve. 2012;45(1):55-9.
171. Lamar K-M, Bogdanovich S, Gardner BB, Gao QQ, Miller T, Earley JU, et al. Overexpression of Latent TGFβ Binding Protein 4 in Muscle Ameliorates Muscular Dystrophy through Myostatin and TGFβ. PLOS Genetics. 2016;12(5):e1006019.
172. Wu Q, Yan T, Chen Y, Chang J, Jiang Y, Zhu D, et al. Integrated Analysis of Expression and Prognostic Values of Acyl-CoA Dehydrogenase short-chain in Colorectal Cancer. International Journal of Medical Sciences. 2021;18(16):3631-43.
173. Chekulayev V, Mado K, Shevchuk I, Koit A, Kaldma A, Klepinin A, et al. Metabolic remodeling in human colorectal cancer and surrounding tissues: alterations in regulation of mitochondrial respiration and metabolic fluxes. Biochem Biophys Rep. 2015;4:111-25.

174. Dzeja P, Terzic A. Adenylate kinase and AMP signaling networks: metabolic monitoring, signal communication and body energy sensing. International journal of molecular sciences. 2009;10(4):1729-72.
175. Thomson DM. The Role of AMPK in the Regulation of Skeletal Muscle Size, Hypertrophy, and Regeneration. International journal of molecular sciences. 2018;19(10):3125.
176. Hu H, Nan J, Sun Y, Zhu D, Xiao C, Wang Y, et al. Electron leak from NDUFA13 within mitochondrial complex I attenuates ischemia-reperfusion injury via dimerized STAT3. Proceedings of the National Academy of Sciences. 2017;114(45):11908-13.
177. Zou S, Tong Q, Liu B, Huang W, Tian Y, Fu X. Targeting STAT3 in Cancer Immunotherapy. Molecular Cancer. 2020;19(1).
178. Correa-de-Araujo R, Addison O, Miljkovic I, Goodpaster BH, Bergman BC, Clark RV, et al. Myosteatosis in the Context of Skeletal Muscle Function Deficit: An Interdisciplinary Workshop at the National Institute on Aging. Frontiers in physiology. 2020;11:963-.
179. Ashpole NM, Sanders JE, Hodges EL, Yan H, Sonntag WE. Growth hormone, insulin-like growth factor-1 and the aging brain. Exp Gerontol. 2015;68:76-81.
180. Smiechowska J, Utech A, Taffet G, Hayes T, Marcelli M, Garcia JM. Adipokines in patients with cancer anorexia and cachexia. J Investig Med. 2010;58(3):554-9.
181. Weryńska B, Kosacka M, Gołecki M, Jankowska R. [Leptin serum levels in cachectic and non-cachectic lung cancer patients]. Pneumonol Alergol Pol. 2009;77(6):500-6.
182. Roeland EJ, Bohlke K, Baracos VE, Bruera E, Fabbro Ed, Dixon S, et al. Management of Cancer Cachexia: ASCO Guideline. Journal of Clinical Oncology. 2020;38(21):2438-53.
183. Unknown article.
184. Baldwin C, Spiro A, Ahern R, Emery PW. Oral Nutritional Interventions in Malnourished Patients With Cancer: A Systematic Review and Meta-Analysis. JNCI: Journal of the National Cancer Institute. 2012;104(5):371-85.
185. Balstad TR, Solheim TS, Strasser F, Kaasa S, Bye A. Dietary treatment of weight loss in patients with advanced cancer and cachexia: A systematic literature review. Critical Reviews in Oncology/Hematology. 2014;91(2):210-21.
186. De Van Der Schueren MAE, Laviano A, Blanchard H, Jourdan M, Arends J, Baracos VE. Systematic review and meta-analysis of the evidence for oral nutritional intervention on nutritional and clinical outcomes during chemo(radio)therapy: current evidence and guidance for design of future trials. Annals of Oncology. 2018;29(5):1141-53.
187. Garcia VR, López-Briz E, Sanchis RC, Perales JLG, Bort-Martí S. Megestrol acetate for treatment of anorexia-cachexia syndrome. Cochrane Database of Systematic Reviews. 2013(3).
188. Yavuzsen T, Davis MP, Walsh D, LeGrand S, Lagman R. Systematic review of the treatment of cancer-associated anorexia and weight loss. Database of Abstracts of Reviews of Effects (DARE): Quality-assessed Reviews [Internet]. 2005.
189. Mavropalias G, Sim M, Taaffe DR, Galvão DA, Spry N, Kraemer WJ, et al. Exercise medicine for cancer cachexia: targeted exercise to counteract mechanisms and treatment side effects. J Cancer Res Clin Oncol. 2022;148(6):1389-406.

Appendix A

Untargeted Serum Proteomics – Aim 2

In addition to the targeted serum proteomics described in Aim 2, untargeted serum proteomics was also completed through the use of isobaric Tandem Mass Tag (TMT) reagents and LC-MS/MS analysis.

Sample selection

40 patients were selected from the discovery cohort that also had sera samples within 90 days of their pre-operative CT scan. Sera samples were from both Dr. Oliver Bathe's biobank in addition to samples from the CLEAR study (provided by ACRB). Specifically, patients were selected based on their body composition status and had to have an independent phenotype of either: just sarcopenia, just myosteatosis, just dense sub-q or no features. For consistency in the cut-points for body composition features and to increase homogeneity of the groups, the lower quartile was utilized as a cut-point for extreme body composition features for each continuous body composition measurement (i.e. SMI, muscle radiodensity, subcutaneous adipose tissue radiodensity) from the discovery cohort (N = 319). All samples were non-metastatic disease, either stages 2 or 3. One sample was mis-classified and was actually a stage 1 and not stage 2, but was still included in the analysis. Each sample was free of inflammatory comorbidities.

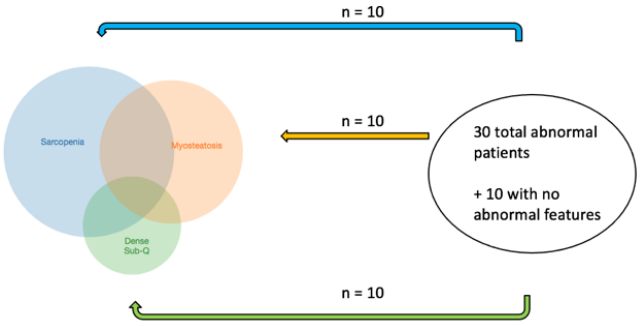

Figure 2.1. Overview of patient selection for TMT proteomics from the discovery cohort

Sample preparation and LC-MS/MS

A subset of the same pre-operative sera utilized for the targeted proteomics were also utilized for this portion of Aim 2 (N = 40). Briefly, the sera utilized were kept in red-top tubes and stored in a -80 freezer. When ready for sample preparation, the sera samples were briefly thawed and vortexed. The samples were then prepared and peptides were labelled the TMT isobaric mass tags. The procedure overview consisted of 1) protein concentration determination with denaturation/precipitation, protein digestion, peptide labelling and a clean-up procedure.

Briefly, the protein concentration of each sample was determined using a BCA Protein Assay Kit. Depending on the concentration of each sample, a specific volume from each sample was extracted in order to have 100ug per condition in new microcentrifuge tubes (N = 40). Each tube was then diluted to 100uL with the dissolution buffer triethyl ammonium bicarbonate (TEAB) to help dissolve proteins in solution. 5uL of 200mM reducing agent TCEP was added to each sample and incubated at 55C for one hour to help denature proteins. 5uL of 200mM iodoacetamide was then added to each sample and incubated in the absence of light to modify sulfur residues. Then 600uL of -20 acetone was added to each solution and kept in a -20 freezer

overnight for protein precipitation. After overnight precipitation, samples were centrifuged and the white protein pellet was the extracted. To start protein digestion, the protein pellet was resuspended in 100uL of 50mM TEAB and a trypsin digest (2.5uL of trypsin per 100ug of protein) was performed overnight at 37C.

For peptide labelling post digestion, TMT Label Reagent (ThermoScientific; 90061) was added to each 100uL sample and let sit for an hour at room temperature. 8uL of 5% hydroxylamine was then added to quench the reaction. Samples were then added to a new centrifuge tubes and were cleaned as an addition step with Solid Phase Extraction Consumable cartridges.

Prepared samples were then submitted for Liquid Chromatography – Tandem Mass Spectrometry (LC-MS/MS) analysis that was conducted through the Southern Alberta Mass Spectrometry Facility and the University of Calgary Cumming School of Medicine. The LC-MS/MS utilized was an Orbitrap Fusion Tribrid Mass Spectrometer (Thermo Fisher Scientific).

Data Analysis

MSstatsTMT

Raw spectral data was processed through MaxQuant. Differential abundance analyses of proteins from the sarcopenia, myosteatosis and dense sub-q phenotypes were all compared to the no phenotype controls. Comparisons were made in the MSstatTMT package in the R environment. Briefly, first the MaxQuant results were uploaded to MSstatsTMT. Protein features

with two quantification values or less were removed and a global normalization at the peptide level was applied. A significance analysis was the applied followed by a correction for multiple comparisons (Benjamini-Hochberg). Volcano plots were generated.

Results

Unfortunately there were no significantly differentially abundant proteins between sarcopenia vs normal, myosteatosis vs normal or dense sub-q vs normal phenotypes after correction for multiple comparison (Figure A.1).

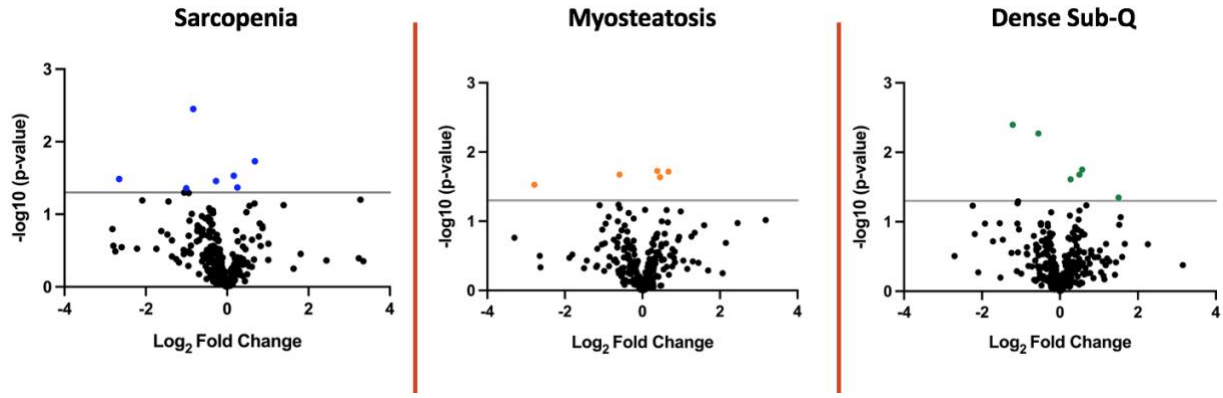

Figure A.1. Volcano plots of differentially abundance proteins but not corrected for multiple comparisons

However, proteins with an positive and negative fold change of 1.5 were submitted to Metascape and some pathways were detected, although these findings are insignificant. Pathways can be observed in Figures A.2 – A.4

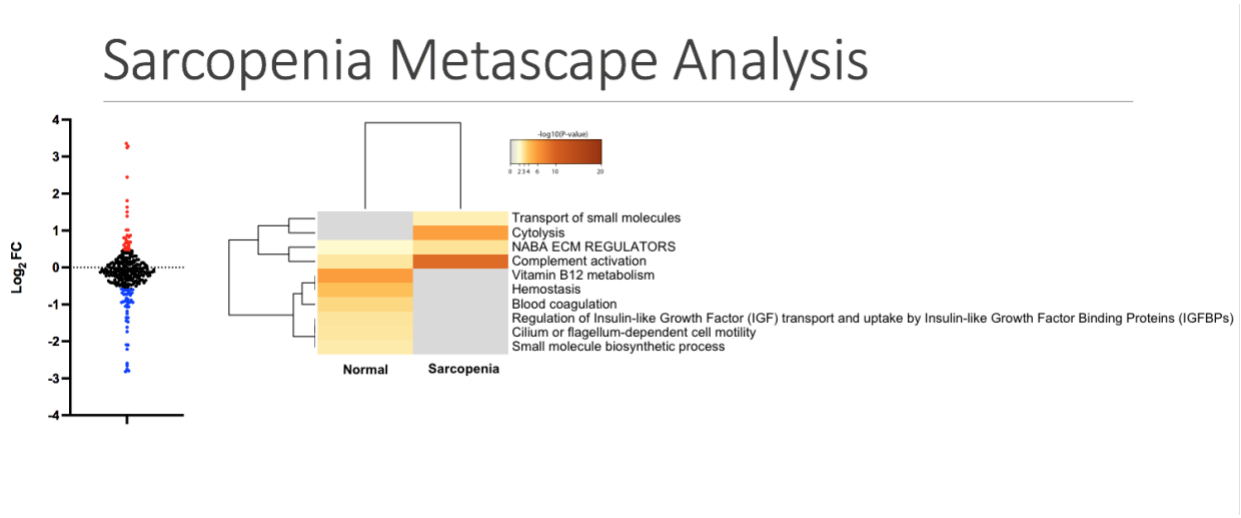

Figure A.2. Sarcopenia metascape analysis

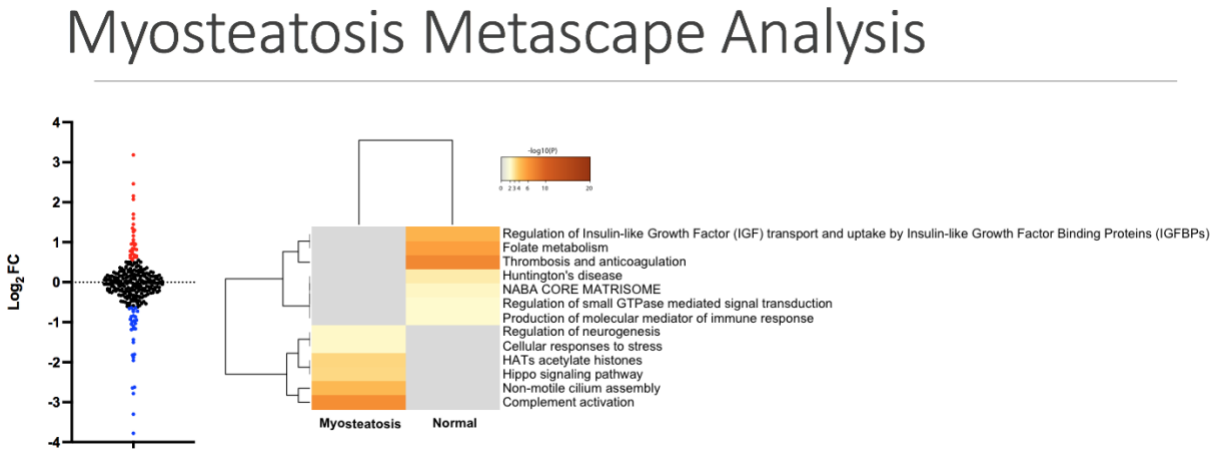

Figure A.3. Myosteatosis metascape analysis

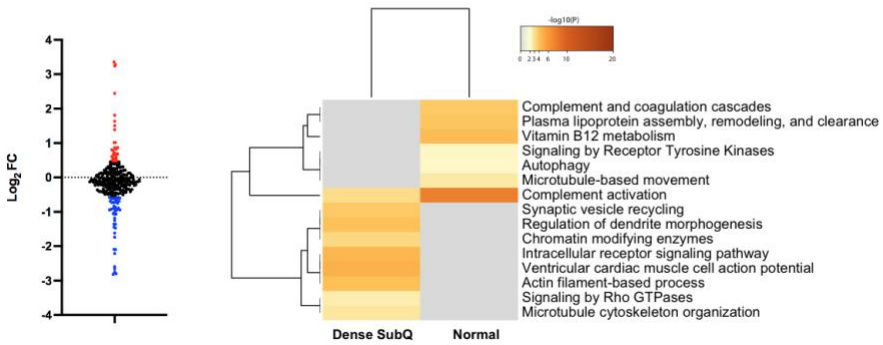

Figure A.4. Dense sub-q metascape analysis